Supplement of Geosci. Model Dev., 15, 5567–5592, 2022
https://doi.org/10.5194/gmd-15-5567-2022-supplement

Geoscientific Model Development
Open Access

Supplement of

Improved representation of plant physiology in the JULES-vn5.6 land surface model: photosynthesis, stomatal conductance and thermal acclimation

Rebecca J. Oliver et al.

Correspondence to: Rebecca J. Oliver (rfu@ceh.ac.uk)

Fig. S1. Simple leaf-level model of gross photosynthesis to show the temperature dependency of gross photosynthesis, V_{cmax} and J_{max} for Collatz (Clz. red) and Farquhar (Fq. blue) with PFT specific parameters (Table 1 and 2) for all 9 JULES PFTs. The dotted vertical lines show the T_{opt} for V_{cmax} and J_{max}.

Theses temperature response curves were produced using simplified Collatz and Farquhar leaf-level models of gross photosynthesis where all environmental variables were fixed (light (300 W m^2 PAR), CO_2 concentration (31 Pa), without water stress), apart from air temperature which was allowed to change in the range of -10 to 50°C. Each PFT was parameterised with PFT specific values from Tables 1 and 2. The resulting temperature dependencies are shown below, and are helpful in interpreting the results of the large scale simulations.

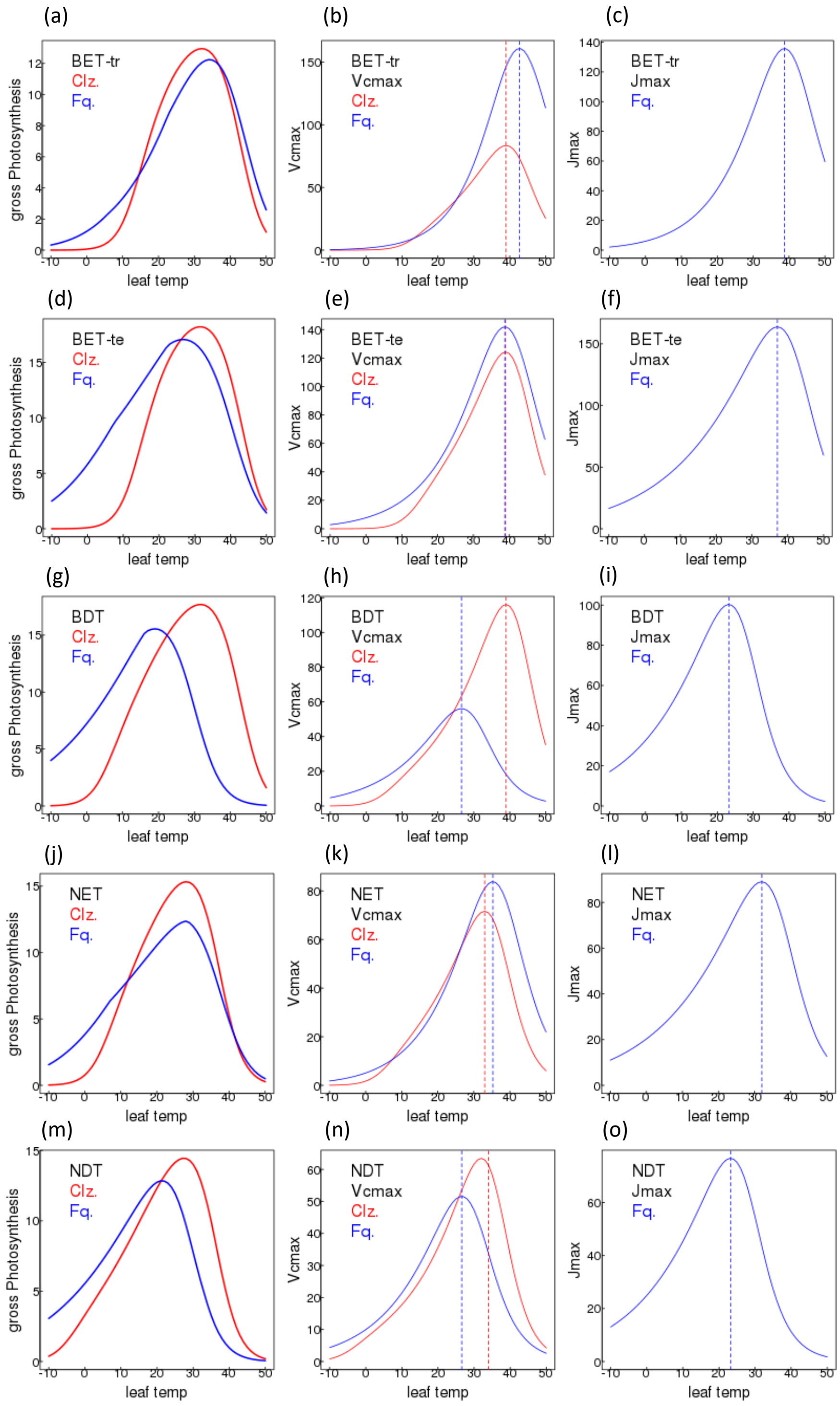

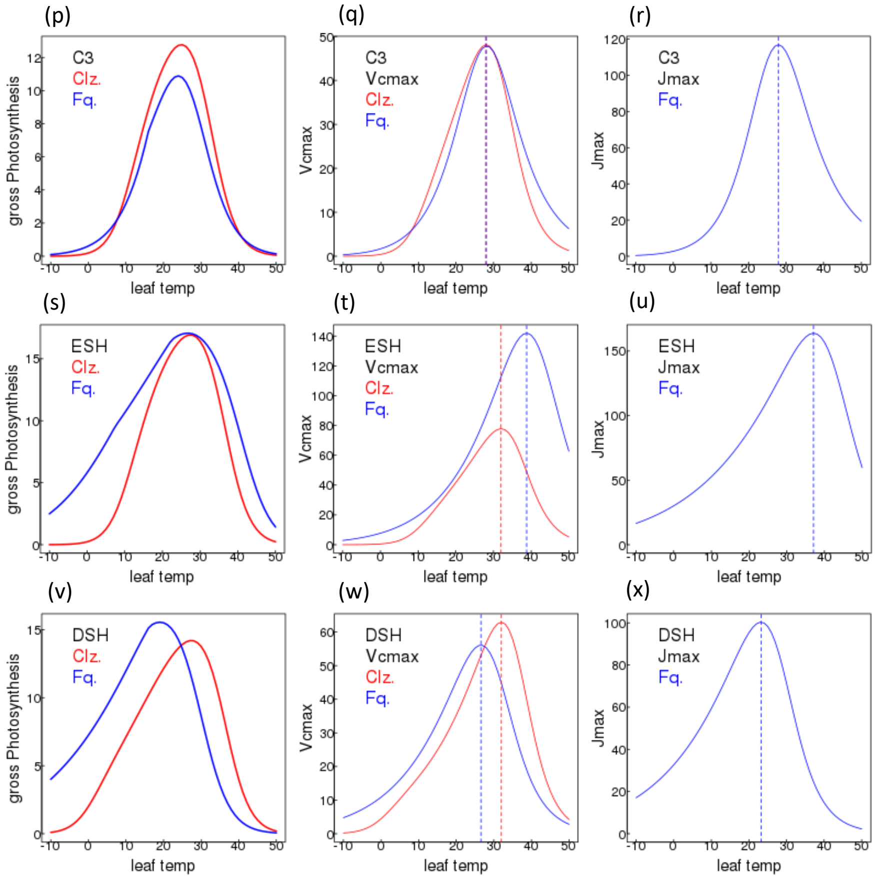

Fig. S2. Location of eddy covariance Flux tower sites used in site-level evaluation. 14 sites were from the Fluxnet tower network (https://fluxnet.org/data/fluxnet2015-dataset/), and three were from the LBA-ECO Flux tower network (https://daac.ornl.gov/LBA/guides/CD32_Brazil_Flux_Network.html)) (Restrepo-Coupe et al., 2013).

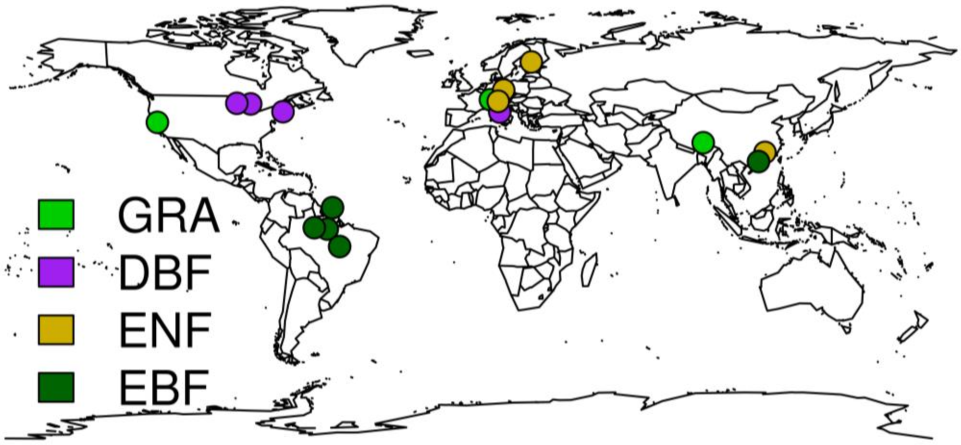

Table S1. Information on Fluxnext 2015 (14 sites) and Brasilflux sites* (3 sites) used for site-level model evaluation. IGBP vegetation types correspond to Evergreen Broadleaved forest & Evergreen Needle leaved Forest (EBF & ENF), Deciduous Broadleaved forest (DBF) and C_3 grasses (GRA). The fractional coverage of each vegetation type as represented by the JULES plant functional types is also given: broad leaved deciduous trees (BDT), evergreen needle leaved trees (NET), C_3 grasses (C3) and broad leaved evergreen tropical (BET-tr). [&] shows where site measured LAI data was available and used in JULES simulations.

Site	Country	Latitude	Longitude	IGBP	JULES fracs	Simulated years
CN_Dan	China	30.50	91.07	GRA	100% C3	2004-2005
AT_Neu[&]	Austria	47.12	11.32	GRA	100% C3	2006-2012
CH_Cha[&]	Switzerland	47.21	8.41	GRA	100% C3	2006-2007
US_Var	USA	38.41	-120.95	GRA	100% C3	2000-2014
US_UMB	USA	45.56	-84.71	DBF	100% BDT	2000-2014
US_Ha1	USA	42.54	-72.17	DBF	100% BDT	1991-2012
IT_CA1	Italy	42.38	12.03	DBF	100% BDT	2011-2014
US_WCr	USA	45.81	-90.08	DBF	100% BDT	1999-2014
FI_Hyy	Finland	61.85	24.30	ENF	100% NET	1996-2014
DE_Tha	Germany	50.96	13.57	ENF	100% NET	1996-2014
CN_Qia	China	26.74	115.06	ENF	100% NET	2003-2005
IT_Ren	Italy	46.59	11.43	ENF	100% NET	1999-2013
GF_Guy[&]	French Guiana	5.28	-52.92	EBF	100 % BET-tr	2007-2009
CN_Din	China	23.17	112.54	EBF	100 % BET-tr	2003-2005
LBA_K83*	Brazil	-3.02	-54.97	EBF	100 % BET-tr	2001-2003
LBA_K34*	Brazil	-2.50	-60.00	EBF	100 % BET-tr	2003-2005
LBA_BAN*	Brazil	-9.82	-50.16	EBF	100 % BET-tr	2004-2006

Fig. S3. Fractional cover of each JULES land cover type.

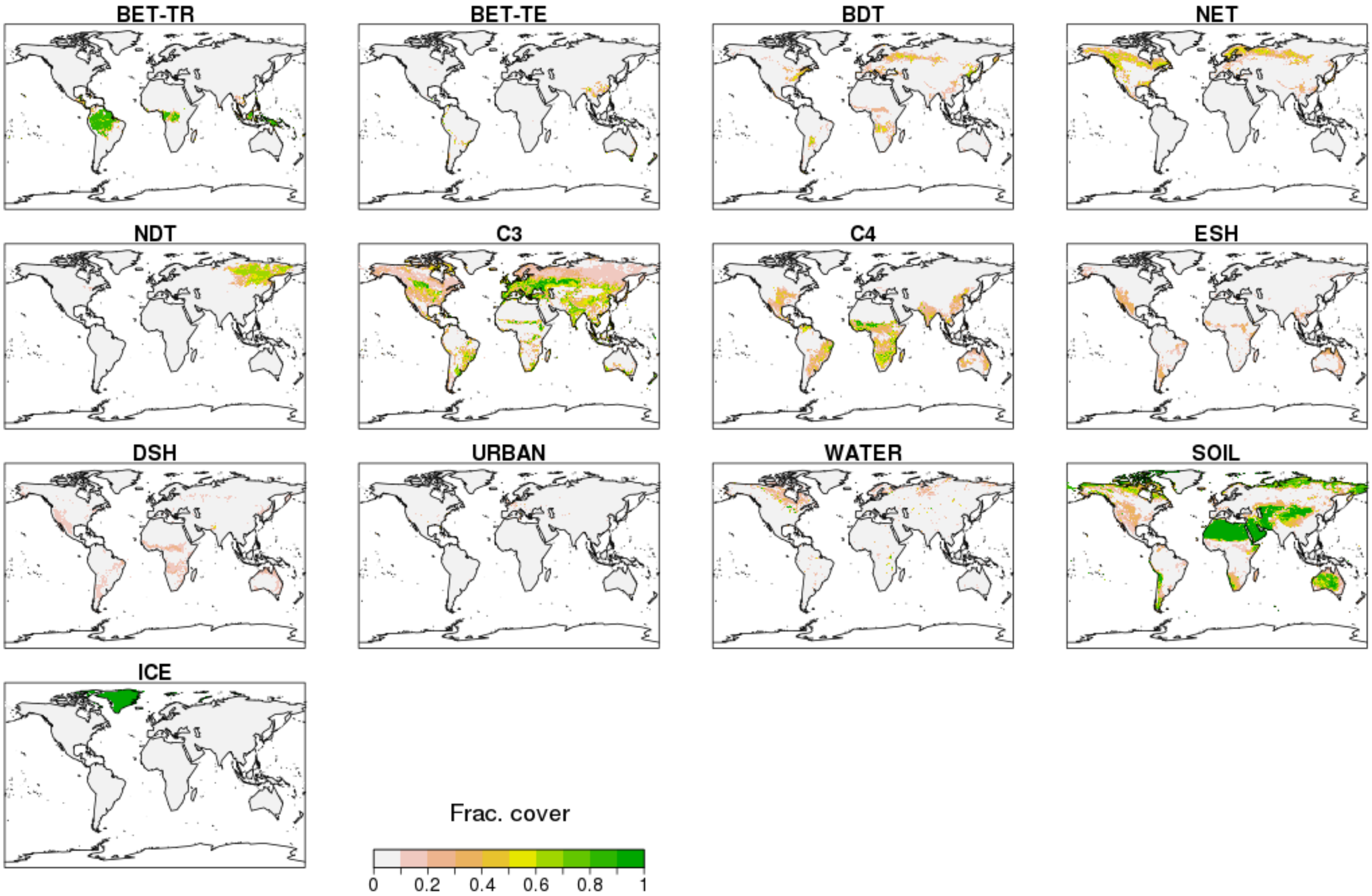

Fig. S4. The mean air temperature (ºC) and precipitation (mm day^{-1}) change by region over the study period (1960 to 2050), and the atmospheric CO_2 concentration (ppm).

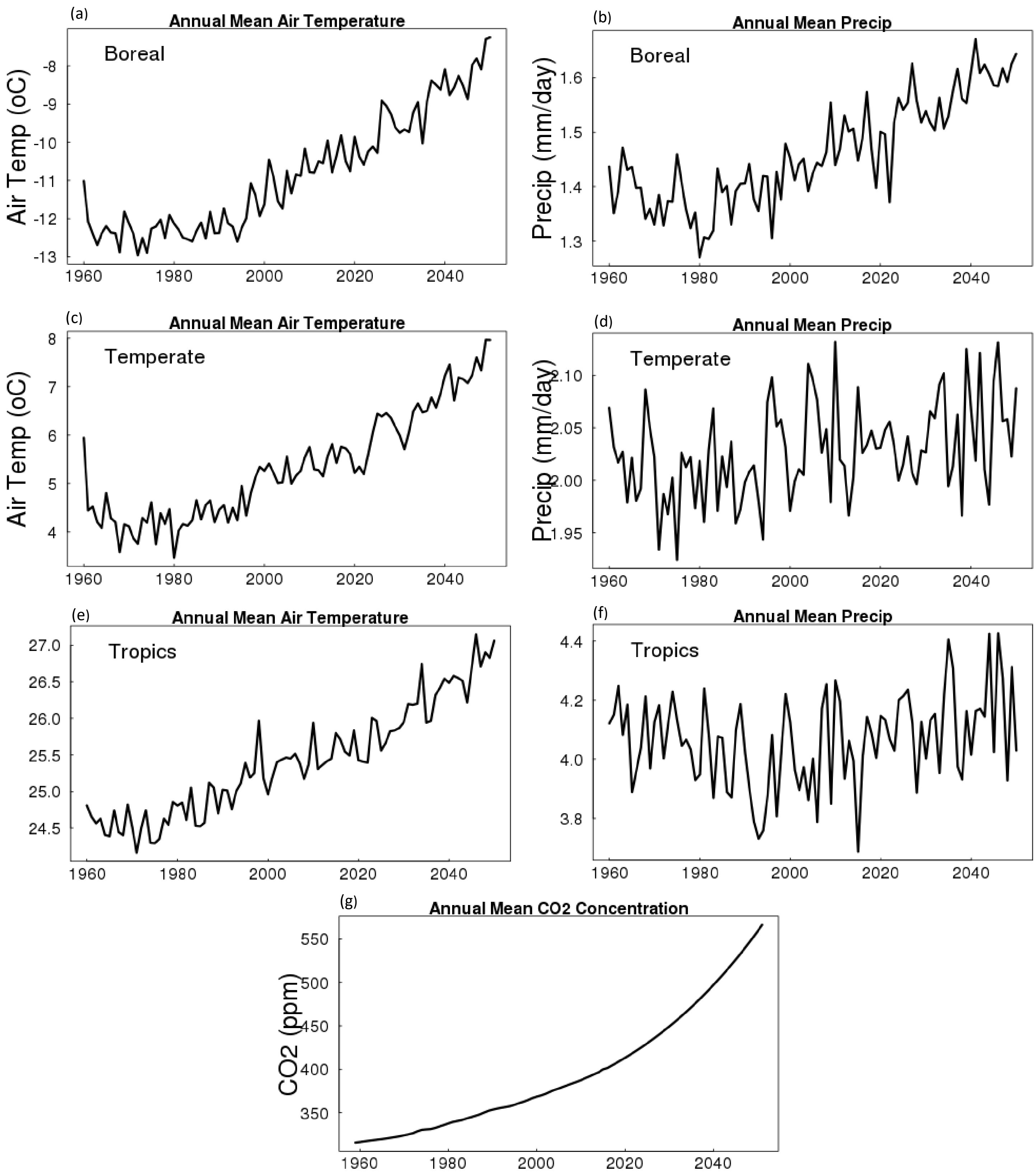

Fig. S5. Mean seasonal diurnal cycles of GPP over the simulation period at the eddy covariance Flux tower sites in Table S1. DJF (December-January-February); MAM (March-April-May); JJA (June-July-August); SON (September-October-November). The black dashed line shows the mean diurnal air temperature (°C same scale as y-axis). The RMSE for each model configuration compared to the observations from Fluxnet are shown at the top of each plot (CJ=Clz.Jac; FJ=Fq.Jac; FM=Fq.Med; AcM=AcKK.Med). These results are summarised in Figure 1 in the main manuscript for MAM and JJA. EBF: Broadleaf evergreen tropical tree, GRA: C_3 grassland, BDT: Broadleaf deciduous tree, NET: Needle leaf evergreen tree.

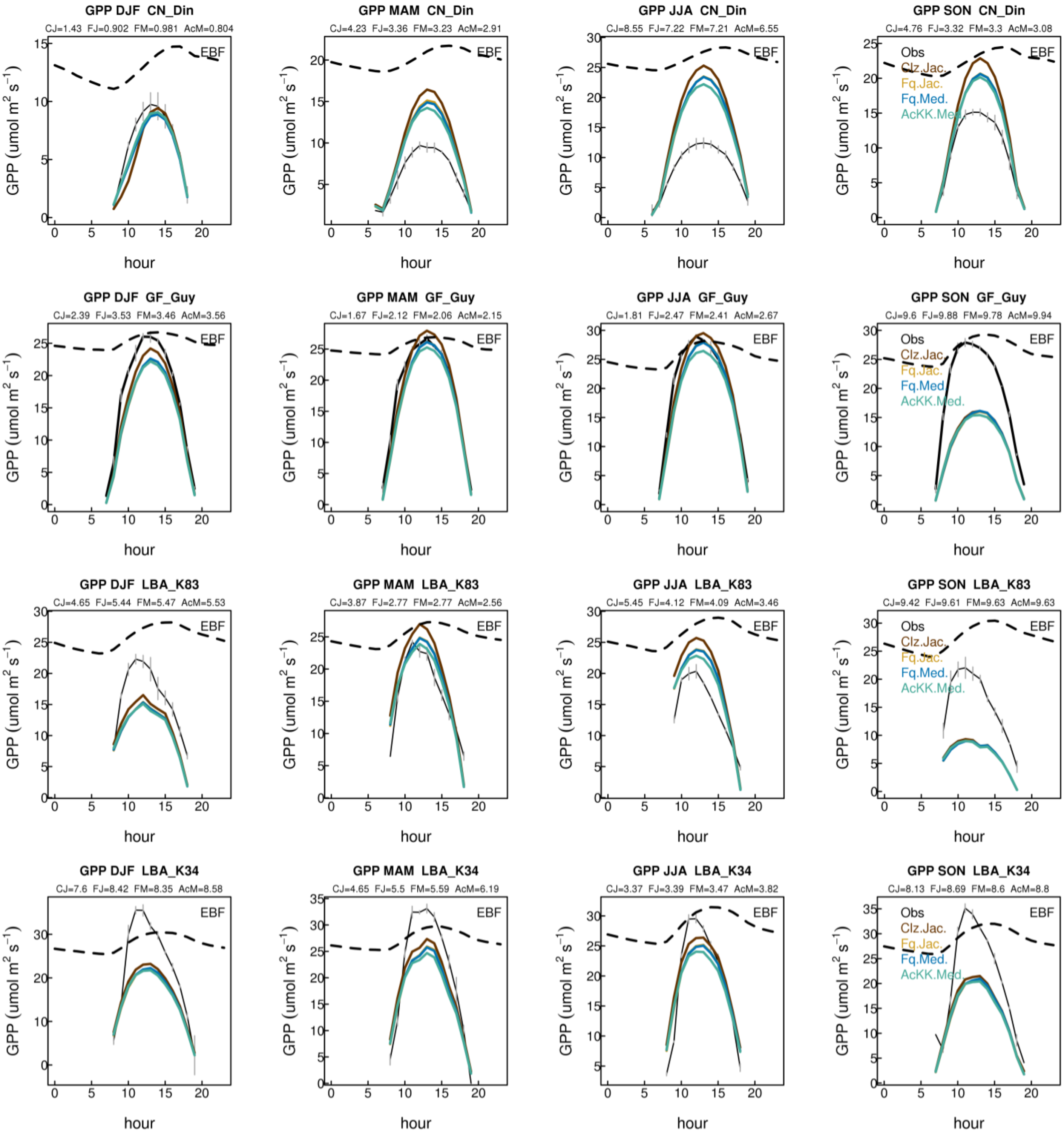

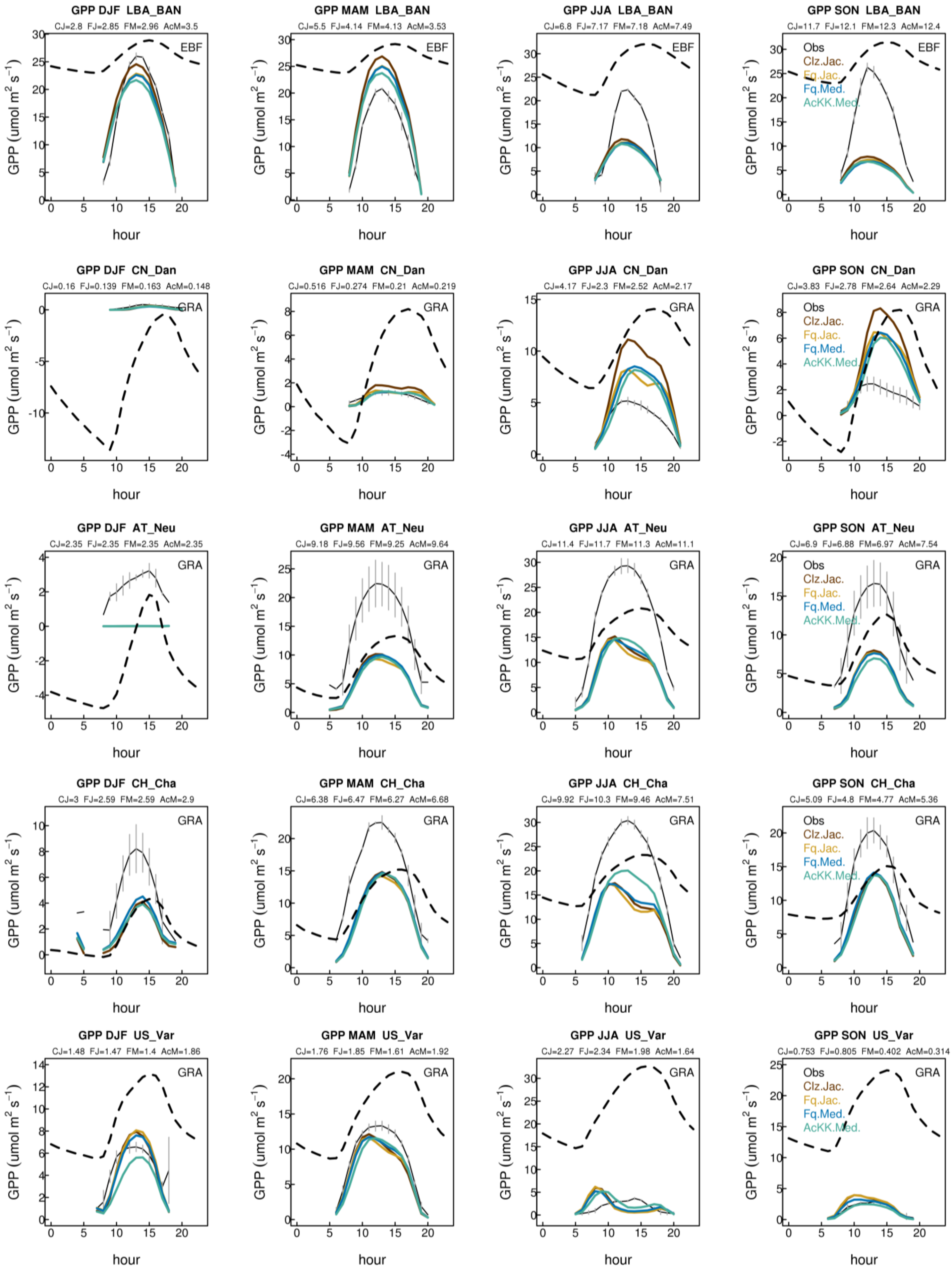
GPP DJF LBA_BAN
CJ=2.8 FJ=2.85 FM=2.96 AcM=3.5
GPP MAM LBA_BAN
CJ=5.5 FJ=4.14 FM=4.13 AcM=3.53
GPP JJA LBA_BAN
CJ=6.8 FJ=7.17 FM=7.18 AcM=7.49
GPP SON LBA_BAN
CJ=11.7 FJ=12.1 FM=12.3 AcM=12.4
EBF
Obs
Clz.Jac.
Fq.Jac.
Fq.Med.
AcKK.Med.
GPP DJF CN_Dan
CJ=0.16 FJ=0.139 FM=0.163 AcM=0.148
GPP MAM CN_Dan
CJ=0.516 FJ=0.274 FM=0.21 AcM=0.219
GPP JJA CN_Dan
CJ=4.17 FJ=2.3 FM=2.52 AcM=2.17
GPP SON CN_Dan
CJ=3.83 FJ=2.78 FM=2.64 AcM=2.29
GPP DJF AT_Neu
CJ=2.35 FJ=2.35 FM=2.35 AcM=2.35
GPP MAM AT_Neu
CJ=9.18 FJ=9.56 FM=9.25 AcM=9.64
GPP JJA AT_Neu
CJ=11.4 FJ=11.7 FM=11.3 AcM=11.1
GPP SON AT_Neu
CJ=6.9 FJ=6.88 FM=6.97 AcM=7.54
GPP DJF CH_Cha
CJ=3 FJ=2.59 FM=2.59 AcM=2.9
GPP MAM CH_Cha
CJ=6.38 FJ=6.47 FM=6.27 AcM=6.68
GPP JJA CH_Cha
CJ=9.92 FJ=10.3 FM=9.46 AcM=7.51
GPP SON CH_Cha
CJ=5.09 FJ=4.8 FM=4.77 AcM=5.36
GPP DJF US_Var
CJ=1.48 FJ=1.47 FM=1.4 AcM=1.86
GPP MAM US_Var
CJ=1.76 FJ=1.85 FM=1.61 AcM=1.92
GPP JJA US_Var
CJ=2.27 FJ=2.34 FM=1.98 AcM=1.64
GPP SON US_Var
CJ=0.753 FJ=0.805 FM=0.402 AcM=0.314
GRA
GPP (umol m2 s-1)
hour

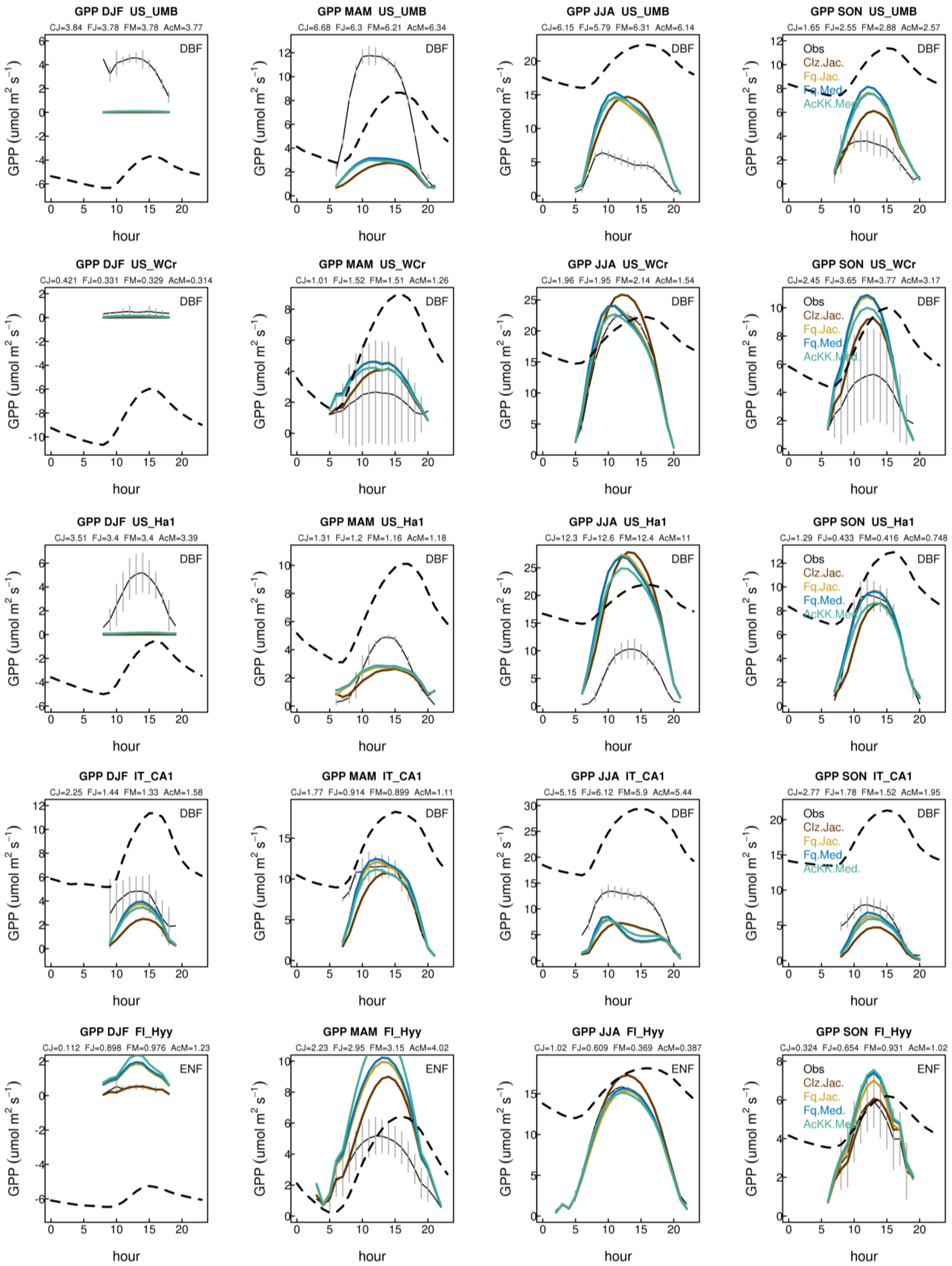
GPP DJF US_UMB
CJ=3.84 FJ=3.78 FM=3.78 AcM=3.77
GPP MAM US_UMB
CJ=6.68 FJ=6.3 FM=6.21 AcM=6.34
GPP JJA US_UMB
CJ=6.15 FJ=5.79 FM=6.31 AcM=6.14
GPP SON US_UMB
CJ=1.65 FJ=2.55 FM=2.88 AcM=2.57
GPP DJF US_WCr
CJ=0.421 FJ=0.331 FM=0.329 AcM=0.314
GPP MAM US_WCr
CJ=1.01 FJ=1.52 FM=1.51 AcM=1.26
GPP JJA US_WCr
CJ=1.96 FJ=1.95 FM=2.14 AcM=1.54
GPP SON US_WCr
CJ=2.45 FJ=3.65 FM=3.77 AcM=3.17
GPP DJF US_Ha1
CJ=3.51 FJ=3.4 FM=3.4 AcM=3.39
GPP MAM US_Ha1
CJ=1.31 FJ=1.2 FM=1.16 AcM=1.18
GPP JJA US_Ha1
CJ=12.3 FJ=12.6 FM=12.4 AcM=11
GPP SON US_Ha1
CJ=1.29 FJ=0.433 FM=0.416 AcM=0.748
GPP DJF IT_CA1
CJ=2.25 FJ=1.44 FM=1.33 AcM=1.58
GPP MAM IT_CA1
CJ=1.77 FJ=0.914 FM=0.899 AcM=1.11
GPP JJA IT_CA1
CJ=5.15 FJ=6.12 FM=5.9 AcM=5.44
GPP SON IT_CA1
CJ=2.77 FJ=1.78 FM=1.52 AcM=1.95
GPP DJF FI_Hyy
CJ=0.112 FJ=0.898 FM=0.976 AcM=1.23
GPP MAM FI_Hyy
CJ=2.23 FJ=2.95 FM=3.15 AcM=4.02
GPP JJA FI_Hyy
CJ=1.02 FJ=0.609 FM=0.369 AcM=0.387
GPP SON FI_Hyy
CJ=0.324 FJ=0.654 FM=0.931 AcM=1.02
DBF
ENF
Obs
Clz.Jac.
Fq.Jac.
Fq.Med.
AcKK.Med.
GPP (umol m2 s-1)
hour

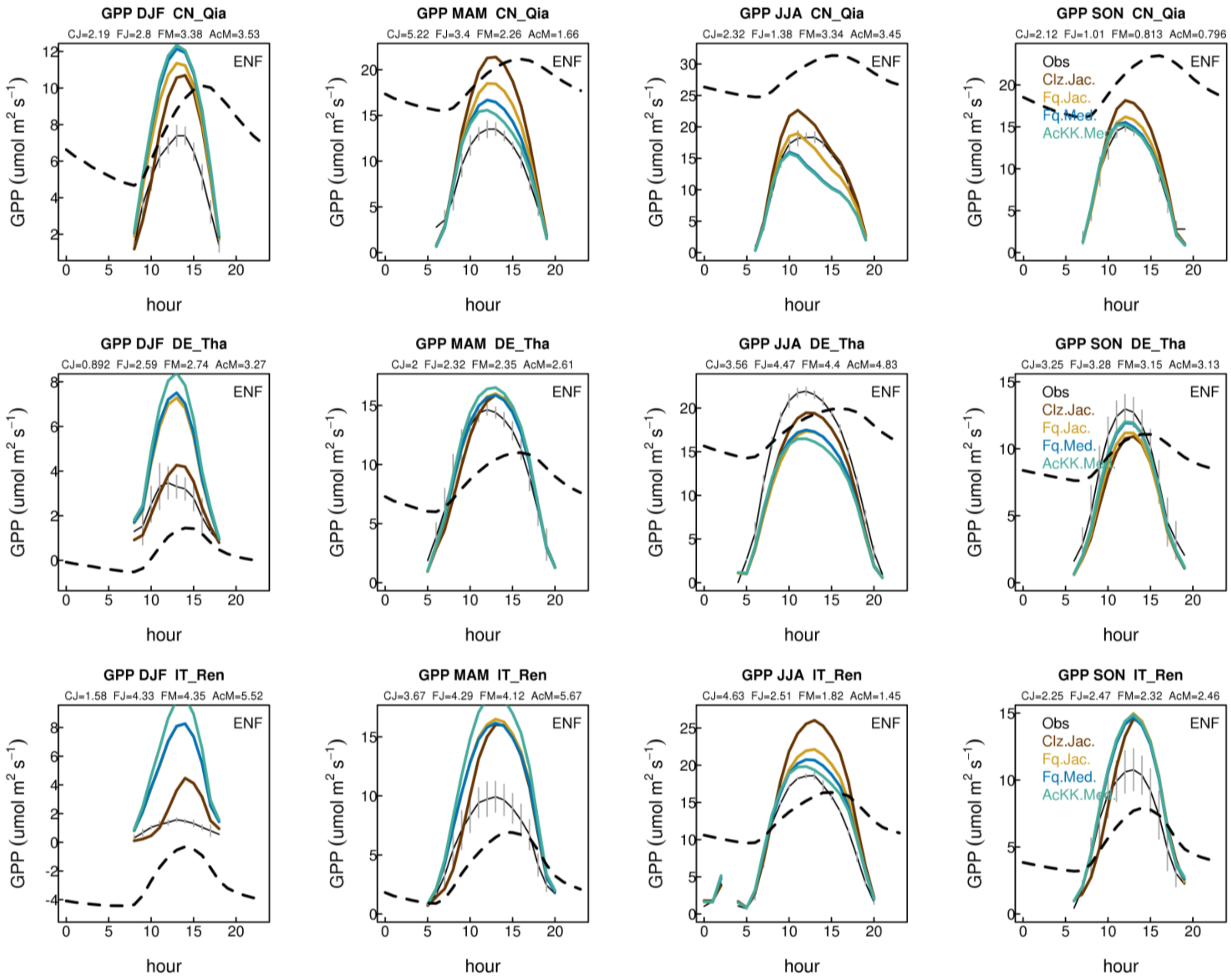
GPP DJF CN_Qia
CJ=2.19 FJ=2.8 FM=3.38 AcM=3.53
GPP MAM CN_Qia
CJ=5.22 FJ=3.4 FM=2.26 AcM=1.66
GPP JJA CN_Qia
CJ=2.32 FJ=1.38 FM=3.34 AcM=3.45
GPP SON CN_Qia
CJ=2.12 FJ=1.01 FM=0.813 AcM=0.796
GPP DJF DE_Tha
CJ=0.892 FJ=2.59 FM=2.74 AcM=3.27
GPP MAM DE_Tha
CJ=2 FJ=2.32 FM=2.35 AcM=2.61
GPP JJA DE_Tha
CJ=3.56 FJ=4.47 FM=4.4 AcM=4.83
GPP SON DE_Tha
CJ=3.25 FJ=3.28 FM=3.15 AcM=3.13
GPP DJF IT_Ren
CJ=1.58 FJ=4.33 FM=4.35 AcM=5.52
GPP MAM IT_Ren
CJ=3.67 FJ=4.29 FM=4.12 AcM=5.67
GPP JJA IT_Ren
CJ=4.63 FJ=2.51 FM=1.82 AcM=1.45
GPP SON IT_Ren
CJ=2.25 FJ=2.47 FM=2.32 AcM=2.46
ENF
Obs
Clz.Jac.
Fq.Jac.
Fq.Med.
AcKK.Med.
GPP (umol m^2 s^{-1})
hour

Fig. S6. Mean seasonal diurnal cycles of EF over the simulation period at the eddy covariance Flux tower sites in Table S1. DJF (December-January-February); MAM (March-April-May); JJA (June-July-August); SON (September-October-November). The RMSE for each model configuration compared to the observations from Fluxnet are shown at the top of each plot (CJ=Clz.Jac; FJ=Fq.Jac; FM=Fq.Med; AcM=AcKK.Med). These results are summarised in Figure 1 in the main manuscript for MAM and JJA. EBF: Broadleaf evergreen tropical tree, GRA: C_3 grassland, BDT: Broadleaf deciduous tree, NET: Needle leaf evergreen tree.

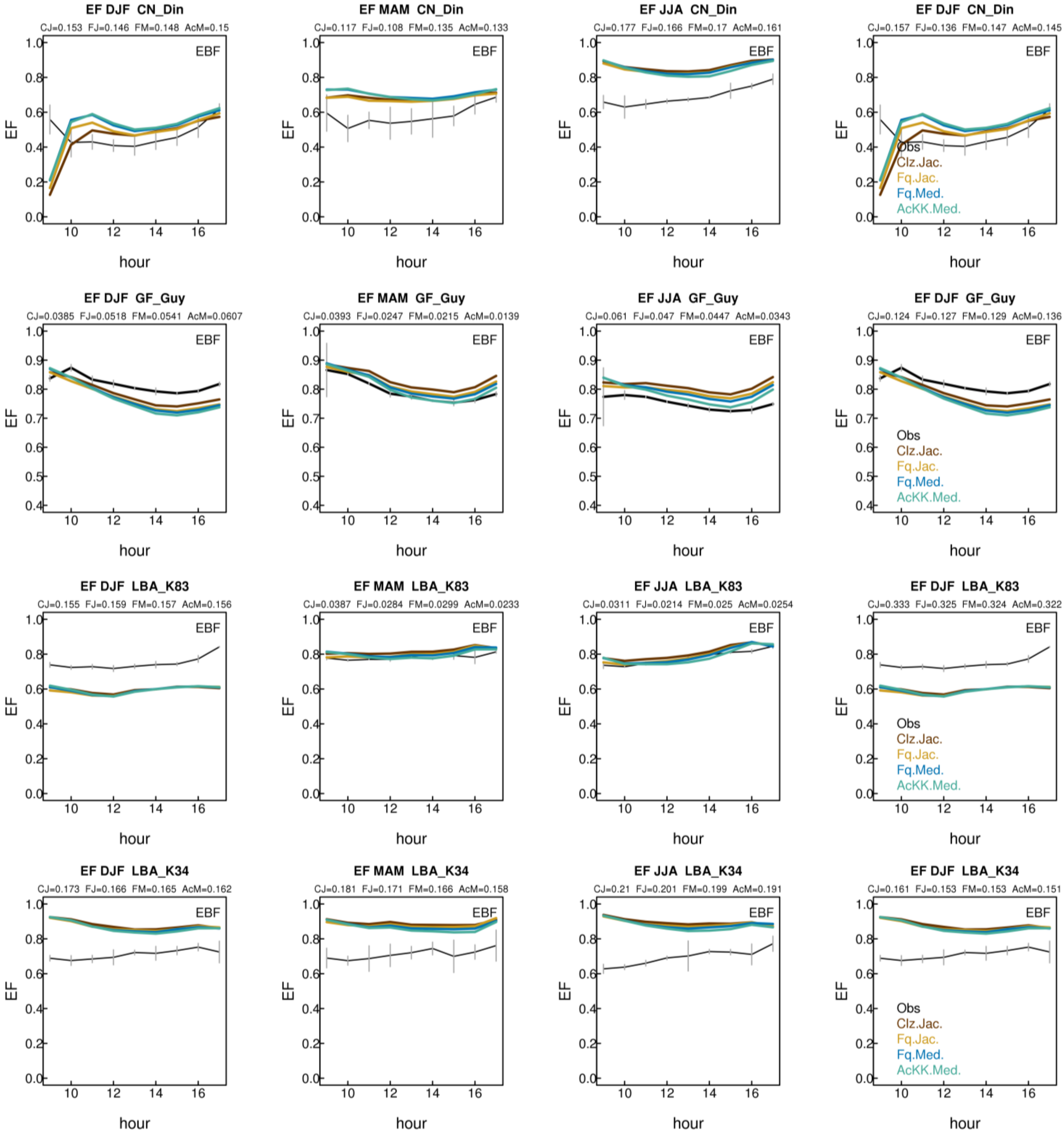

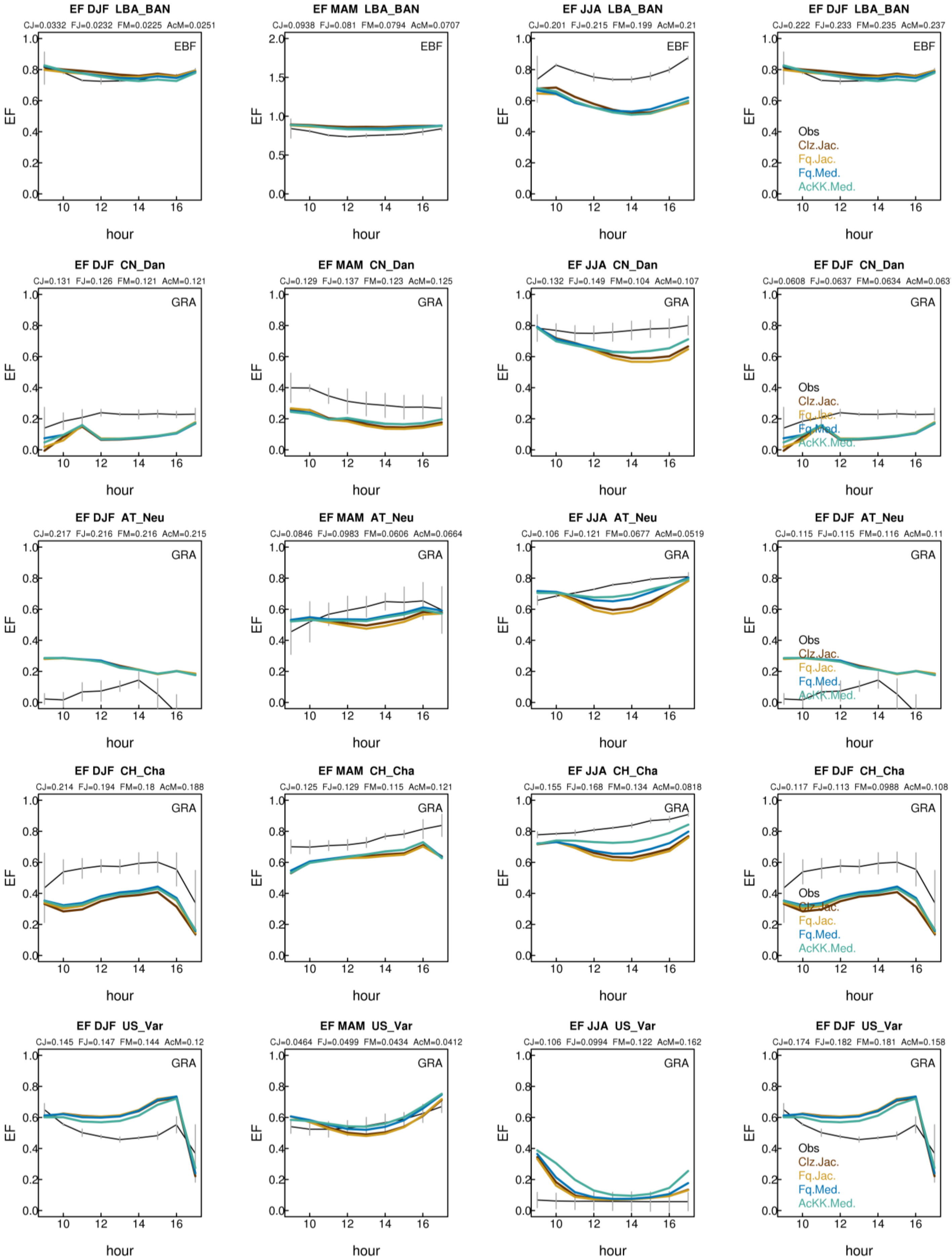
EF DJF LBA_BAN
CJ=0.0332 FJ=0.0232 FM=0.0225 AcM=0.0251
EBF
EF MAM LBA_BAN
CJ=0.0938 FJ=0.081 FM=0.0794 AcM=0.0707
EBF
EF JJA LBA_BAN
CJ=0.201 FJ=0.215 FM=0.199 AcM=0.21
EBF
EF DJF LBA_BAN
CJ=0.222 FJ=0.233 FM=0.235 AcM=0.237
EBF
EF DJF CN_Dan
CJ=0.131 FJ=0.126 FM=0.121 AcM=0.121
GRA
EF MAM CN_Dan
CJ=0.129 FJ=0.137 FM=0.123 AcM=0.125
GRA
EF JJA CN_Dan
CJ=0.132 FJ=0.149 FM=0.104 AcM=0.107
GRA
EF DJF CN_Dan
CJ=0.0608 FJ=0.0637 FM=0.0634 AcM=0.063
GRA
EF DJF AT_Neu
CJ=0.217 FJ=0.216 FM=0.216 AcM=0.215
GRA
EF MAM AT_Neu
CJ=0.0846 FJ=0.0983 FM=0.0606 AcM=0.0664
GRA
EF JJA AT_Neu
CJ=0.106 FJ=0.121 FM=0.0677 AcM=0.0519
GRA
EF DJF AT_Neu
CJ=0.115 FJ=0.115 FM=0.116 AcM=0.11
GRA
EF DJF CH_Cha
CJ=0.214 FJ=0.194 FM=0.18 AcM=0.188
GRA
EF MAM CH_Cha
CJ=0.125 FJ=0.129 FM=0.115 AcM=0.121
GRA
EF JJA CH_Cha
CJ=0.155 FJ=0.168 FM=0.134 AcM=0.0818
GRA
EF DJF CH_Cha
CJ=0.117 FJ=0.113 FM=0.0988 AcM=0.108
GRA
EF DJF US_Var
CJ=0.145 FJ=0.147 FM=0.144 AcM=0.12
GRA
EF MAM US_Var
CJ=0.0464 FJ=0.0499 FM=0.0434 AcM=0.0412
GRA
EF JJA US_Var
CJ=0.106 FJ=0.0994 FM=0.122 AcM=0.162
GRA
EF DJF US_Var
CJ=0.174 FJ=0.182 FM=0.181 AcM=0.158
GRA
EF
hour
Obs
Clz.Jac.
Fq.Jac.
Fq.Med.
AcKK.Med.

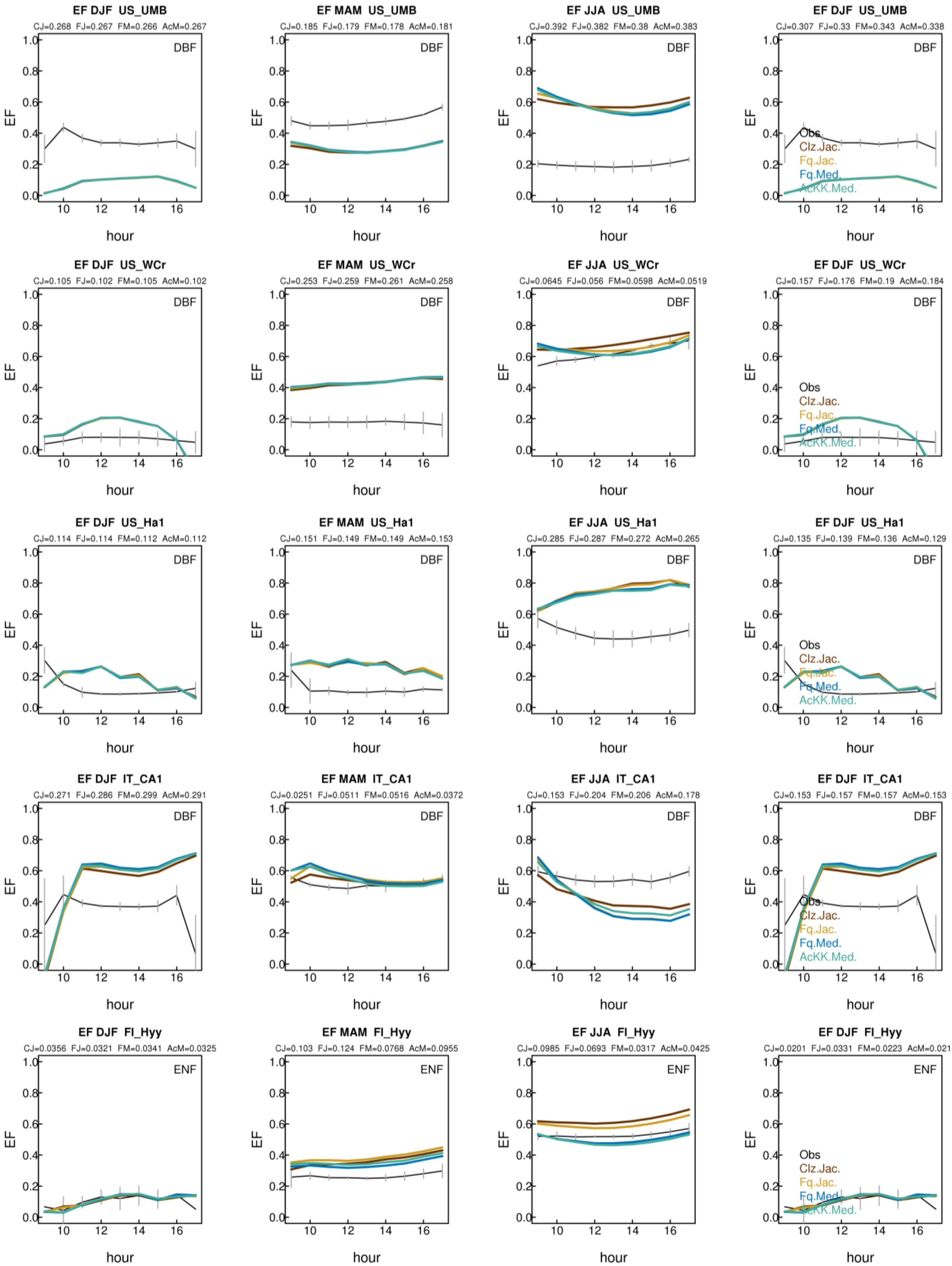
EF DJF US_UMB
CJ=0.268 FJ=0.267 FM=0.266 AcM=0.267
DBF
EF MAM US_UMB
CJ=0.185 FJ=0.179 FM=0.178 AcM=0.181
DBF
EF JJA US_UMB
CJ=0.392 FJ=0.382 FM=0.38 AcM=0.383
DBF
EF DJF US_UMB
CJ=0.307 FJ=0.33 FM=0.343 AcM=0.338
DBF
Obs.
Clz.Jac.
Fq.Jac.
Fq.Med.
AcKK.Med.
EF DJF US_WCr
CJ=0.105 FJ=0.102 FM=0.105 AcM=0.102
DBF
EF MAM US_WCr
CJ=0.253 FJ=0.259 FM=0.261 AcM=0.258
DBF
EF JJA US_WCr
CJ=0.0645 FJ=0.056 FM=0.0598 AcM=0.0519
DBF
EF DJF US_WCr
CJ=0.157 FJ=0.176 FM=0.19 AcM=0.184
DBF
Obs
Clz.Jac.
Fq.Jac.
Fq.Med.
AcKK.Med.
EF DJF US_Ha1
CJ=0.114 FJ=0.114 FM=0.112 AcM=0.112
DBF
EF MAM US_Ha1
CJ=0.151 FJ=0.149 FM=0.149 AcM=0.153
DBF
EF JJA US_Ha1
CJ=0.285 FJ=0.287 FM=0.272 AcM=0.265
DBF
EF DJF US_Ha1
CJ=0.135 FJ=0.139 FM=0.136 AcM=0.129
DBF
Obs
Clz.Jac.
Fq.Jac.
Fq.Med.
AcKK.Med.
EF DJF IT_CA1
CJ=0.271 FJ=0.286 FM=0.299 AcM=0.291
DBF
EF MAM IT_CA1
CJ=0.0251 FJ=0.0511 FM=0.0516 AcM=0.0372
DBF
EF JJA IT_CA1
CJ=0.153 FJ=0.204 FM=0.206 AcM=0.178
DBF
EF DJF IT_CA1
CJ=0.153 FJ=0.157 FM=0.157 AcM=0.153
DBF
Obs
Clz.Jac.
Fq.Jac.
Fq.Med.
AcKK.Med.
EF DJF FI_Hyy
CJ=0.0356 FJ=0.0321 FM=0.0341 AcM=0.0325
ENF
EF MAM FI_Hyy
CJ=0.103 FJ=0.124 FM=0.0768 AcM=0.0955
ENF
EF JJA FI_Hyy
CJ=0.0985 FJ=0.0693 FM=0.0317 AcM=0.0425
ENF
EF DJF FI_Hyy
CJ=0.0201 FJ=0.0331 FM=0.0223 AcM=0.021
ENF
Obs
Clz.Jac.
Fq.Jac.
Fq.Med.
AcKK.Med.
EF
hour

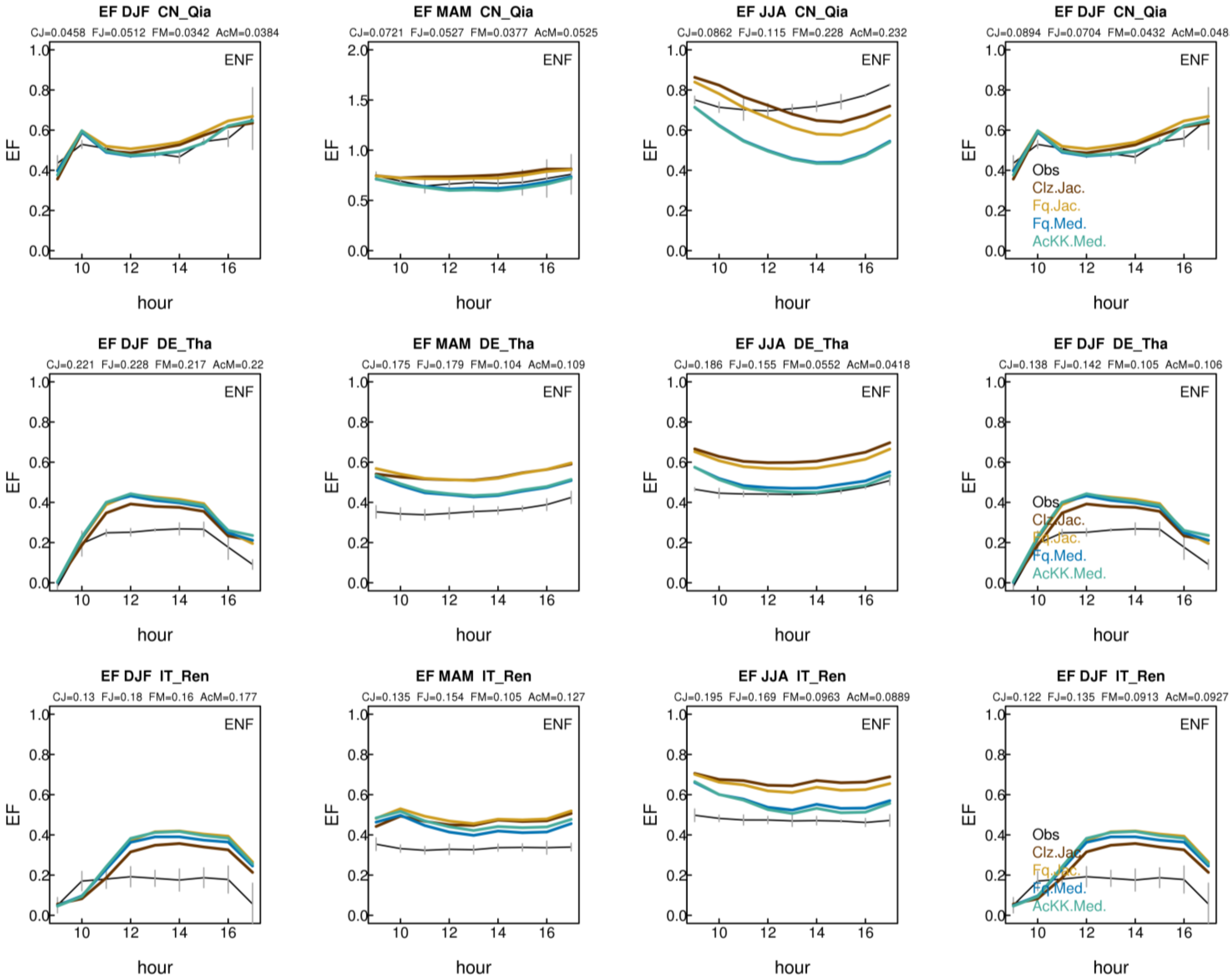

EF DJF CN_Qia
CJ=0.0458 FJ=0.0512 FM=0.0342 AcM=0.0384
EF MAM CN_Qia
CJ=0.0721 FJ=0.0527 FM=0.0377 AcM=0.0525
EF JJA CN_Qia
CJ=0.0862 FJ=0.115 FM=0.228 AcM=0.232
EF DJF CN_Qia
CJ=0.0894 FJ=0.0704 FM=0.0432 AcM=0.048
EF DJF DE_Tha
CJ=0.221 FJ=0.228 FM=0.217 AcM=0.22
EF MAM DE_Tha
CJ=0.175 FJ=0.179 FM=0.104 AcM=0.109
EF JJA DE_Tha
CJ=0.186 FJ=0.155 FM=0.0552 AcM=0.0418
EF DJF DE_Tha
CJ=0.138 FJ=0.142 FM=0.105 AcM=0.106
EF DJF IT_Ren
CJ=0.13 FJ=0.18 FM=0.16 AcM=0.177
EF MAM IT_Ren
CJ=0.135 FJ=0.154 FM=0.105 AcM=0.127
EF JJA IT_Ren
CJ=0.195 FJ=0.169 FM=0.0963 AcM=0.0889
EF DJF IT_Ren
CJ=0.122 FJ=0.135 FM=0.0913 AcM=0.0927
ENF
EF
hour
Obs
Clz.Jac.
Fq.Jac.
Fq.Med.
AcKK.Med.

Fig. S7. Sensitivity of simulated intercellular CO2 concentration (ci) to leaf-level specific humidity deficit (DQC) for the Jacobs and Medlyn g_s models at LBA-K34 (left-hand panel of plots) and FI-Hyy (right-hand panel of plots) FLUXNET sites.

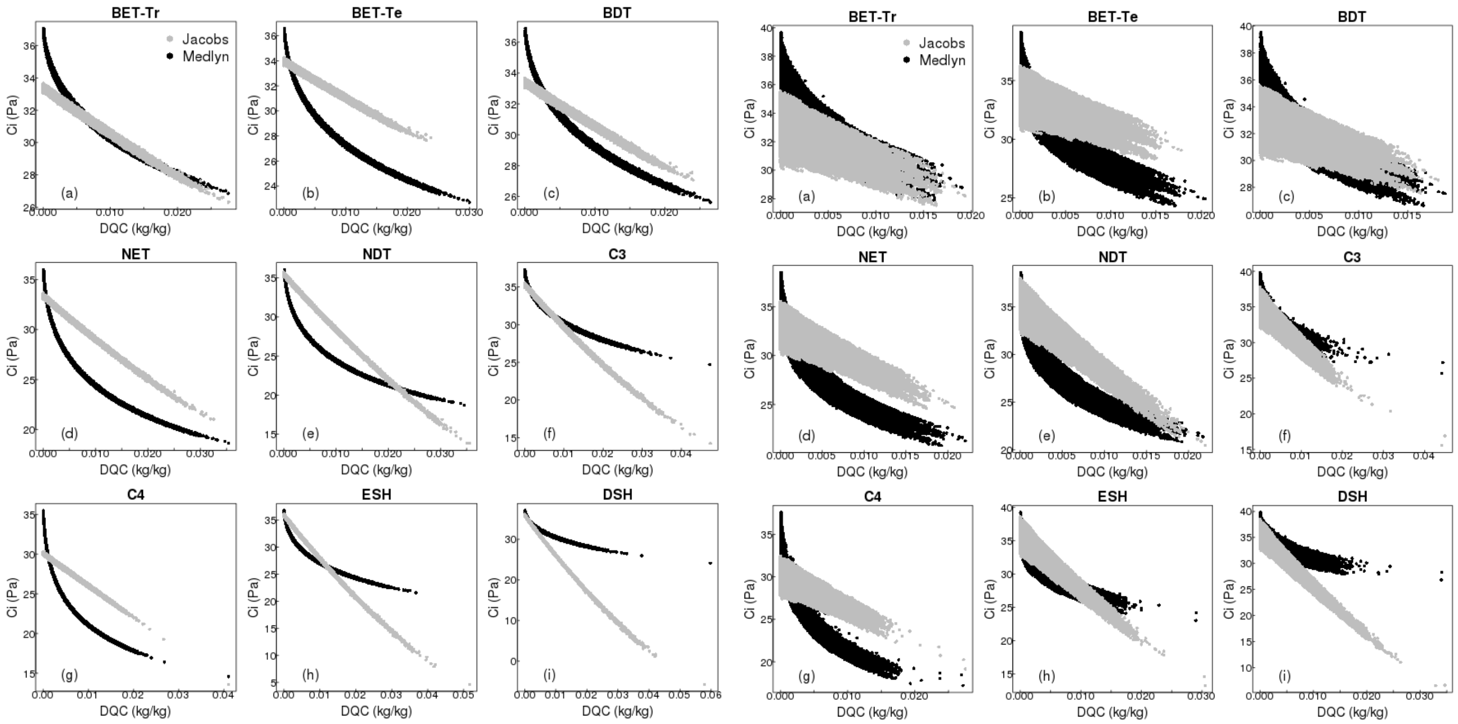

Fig. S8. Absolute mean GPP (a, d, g, j), LE (b, e, h, k), and H (c, f, i, l) simulated by the different JULES model configurations in JJA under present-day (WFDEI) meteorological conditions over the period 2002 to 2012.

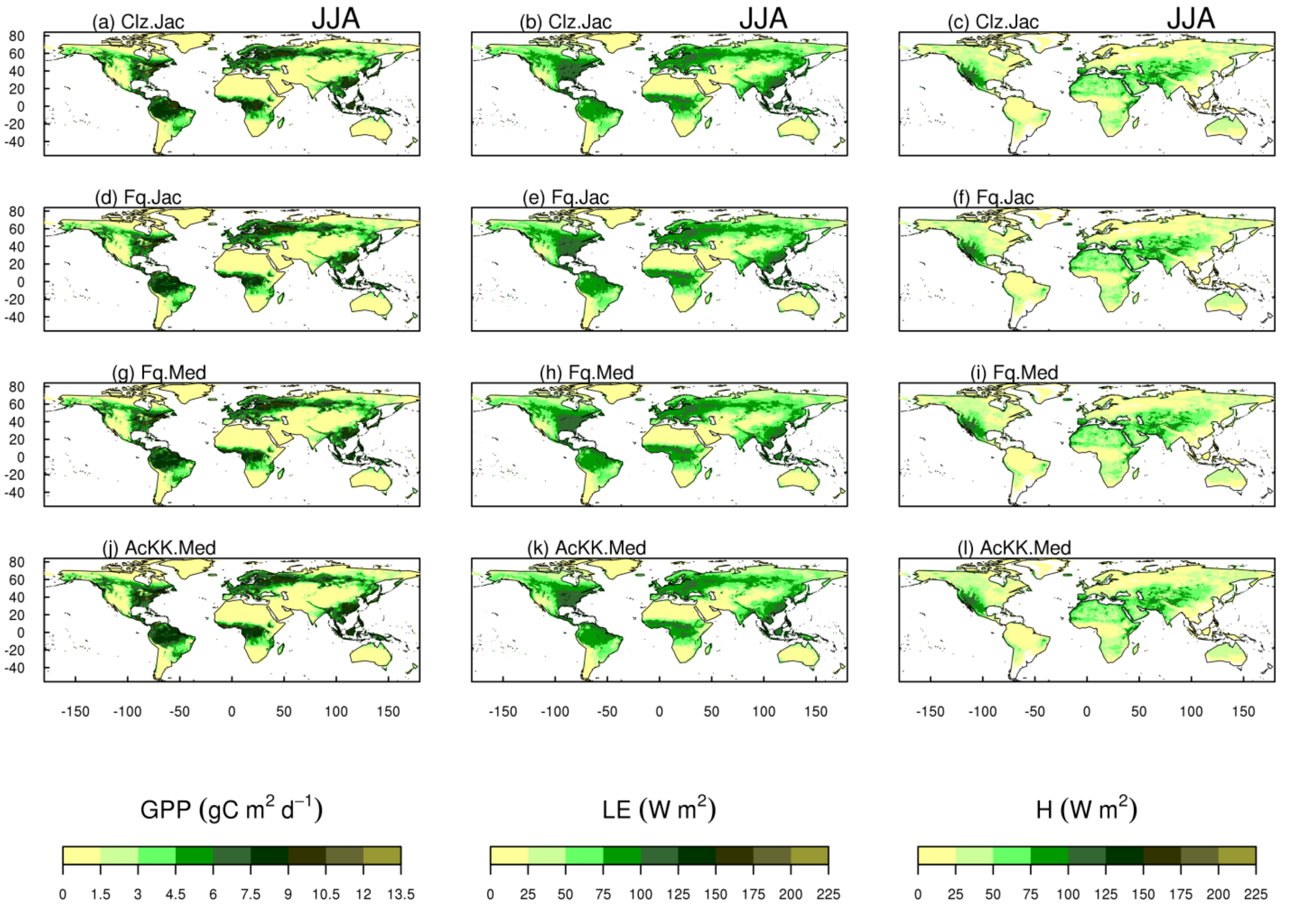

Fig. S9. Absolute mean GPP (a, d, g, j), LE (b, e, h, k), and H (c, f, i, l) simulated by the different JULES model configurations in DJF under present-day (WFDEI) meteorological conditions over the period 2002 to 2012.

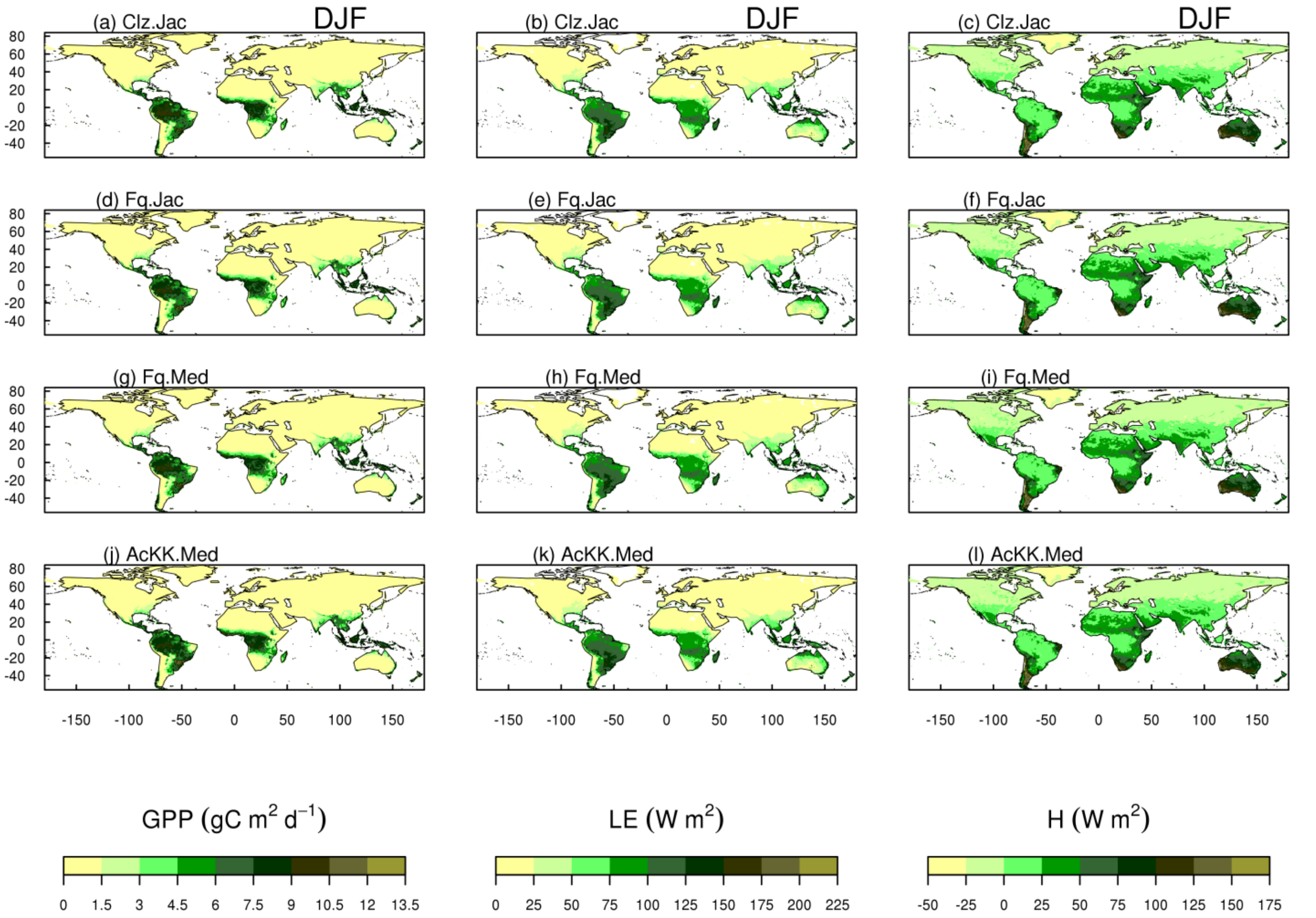

Fig. S10. Differences between JULES modelled GPP, latent (LE) and sensible heat (H) for the different JULES model configurations in December-January-February (DJF). For each variable the mean over the period 2002 to 2012 is used.

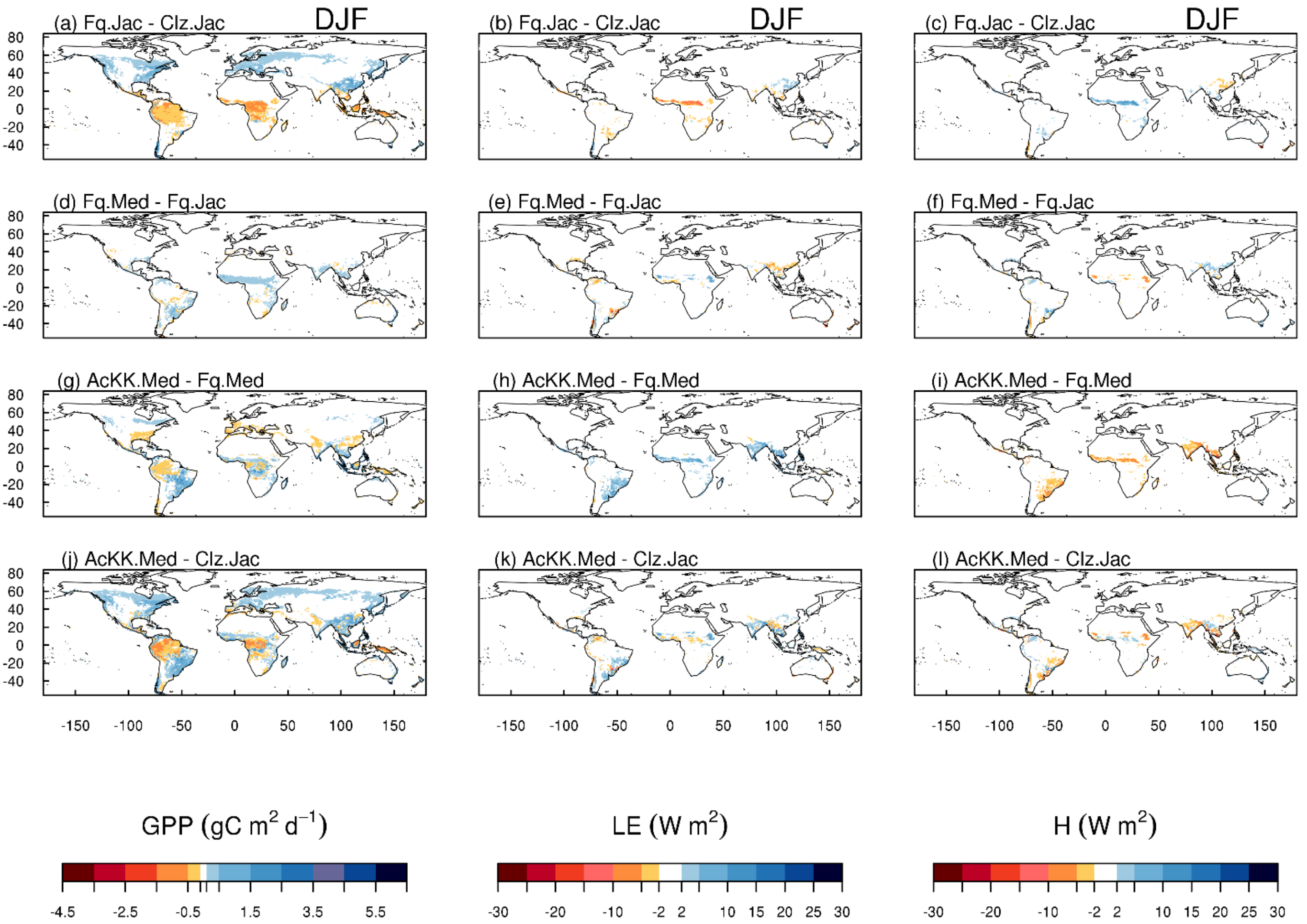

Table S2. Seasonal mean (and annual mean) global GPP (Pg C) of each JULES model configuration and global GPP products FluxCom and MOD17.

	GPP Pg C season^{-1}				Pg C yr^{-1}
	JJA	MAM	SON	DJF	Annual
FluxCom	44.7	32.5	29.4	25.7	132.3
MOD17	39.0	26.8	25.5	20.4	111.7
Clz.Jac	42.2	28.8	34.5	24.8	130.3
Fq.Jac	41.7	29.1	34.4	25.0	130.2
Fq.Med	42.0	29.5	34.5	25.3	131.3
AcKK.Med	43.1	30.9	35.4	26.3	135.7

Table S3. Seasonal mean ET of each JULES model configuration and global ET products from FluxCom and GLEAM.

	ET mm season^{-1}				mm yr^{-1}
	JJA	MAM	SON	DJF	Annual
FluxCom	203.32	148.12	114.66	90.90	557.00
Gleam	199.64	143.52	113.75	92.70	549.61
Clz.Jac	194.12	126.04	153.79	100.80	574.75
Fq.Jac	192.28	125.12	153.79	99.90	571.09
Fq.Med	190.44	125.12	151.97	99.00	566.53
AcKK.Med	192.28	126.04	152.88	100.80	572.00

Table S4. Latitude mean RMSE by region and season for GPP (gC m^2 d^{-1}) simulated by each model configuration compared to the FluxCom global GPP product.

Tropics: -20S TO 20N	RMSE (GPP gC m^2 d^{-1})			
	JJA	MAM	SON	DJF
Clz.Jac	1.45	1.28	1.08	1.31
Fq.Jac	**1.33**	**1.10**	**0.99**	**1.25**
Fq.Med	1.40	1.14	1.00	1.30
AcKK.Med	1.38	1.38	1.27	1.32
Sub-tropics: 20N to 30N				
Clz.Jac	0.94	0.41	1.27	**1.03**
Fq.Jac	0.97	0.32	1.18	1.19
Fq.Med	1.00	**0.26**	**1.14**	1.23
AcKK.Med	**0.61**	0.32	1.92	1.22
Sub-tropics: -20S to -30S				
Clz.Jac	**0.23**	0.23	0.58	1.35
Fq.Jac	0.30	**0.22**	0.52	1.35
Fq.Med	0.34	0.29	**0.46**	1.29
AcKK.Med	0.30	0.46	0.49	**1.28**
Temperate N: 30N to 60N				
Clz.Jac	**0.61**	0.89	**1.24**	**0.11**
Fq.Jac	0.72	0.70	1.34	0.26
Fq.Med	0.72	0.70	1.34	0.26
AcKK.Med	0.66	**0.66**	1.28	0.25
Temperate S: -30S to -60S				
Clz.Jac	0.24	**0.60**	0.93	0.62
Fq.Jac	0.19	0.91	0.47	0.66
Fq.Med	**0.18**	0.87	**0.46**	0.62
AcKK.Med	0.19	0.81	0.51	**0.57**
Boreal: 60N+				
Clz.Jac	0.95	0.25	**0.86**	**0.13**
Fq.Jac	0.94	0.15	0.98	0.15
Fq.Med	**0.93**	0.15	1.00	0.15
AcKK.Med	0.95	**0.06**	0.95	0.16

Table S5. Latitude mean RMSE by region and season for GPP (gC m^2 d^{-1}) simulated by each model configuration compared to the MOD17 global GPP product.

Tropics: -20S TO 20N	RMSE (GPP gC m^2 d^{-1})			
	JJA	MAM	SON	DJF
Clz.Jac	0.99	1.08	1.35	1.09
Fq.Jac	**0.80**	**0.82**	**1.20**	**0.90**
Fq.Med	0.86	0.88	1.23	0.97
AcKK.Med	0.99	1.15	1.51	1.12
Sub-tropics: 20N to 30N				
Clz.Jac	0.34	0.59	1.26	**0.45**
Fq.Jac	0.29	**0.50**	1.17	0.68
Fq.Med	**0.26**	0.55	**1.12**	0.71
AcKK.Med	0.52	0.51	1.90	0.69
Sub-tropics: -20S to -30S				
Clz.Jac	0.50	0.30	0.67	0.47
Fq.Jac	0.39	0.27	0.60	0.47
Fq.Med	**0.36**	**0.25**	**0.55**	0.41
AcKK.Med	0.41	0.33	0.58	**0.30**
Temperate N: 30N to 60N				
Clz.Jac	**0.49**	0.77	**0.91**	**0.07**
Fq.Jac	0.50	0.57	1.02	0.22
Fq.Med	0.52	0.57	1.03	0.22
AcKK.Med	0.54	**0.54**	0.96	0.21
Temperate S: -30S to -60S				
Clz.Jac	0.41	0.58	1.20	0.73
Fq.Jac	0.35	0.83	0.75	0.60
Fq.Med	**0.34**	0.78	**0.74**	0.54
AcKK.Med	0.39	**0.73**	0.79	**0.52**
Boreal: 60N+				
Clz.Jac	1.32	0.22	**0.71**	**0.01**
Fq.Jac	1.27	0.12	0.83	0.03
Fq.Med	1.27	0.12	0.84	0.03
AcKK.Med	**1.26**	**0.03**	0.80	0.04

Table S6. Latitude mean RMSE by region and season for ET (mm d^{-1}) simulated by each model configuration compared to the FluxCom global ET product.

Tropics: -20S TO 20N	RMSE (ET mm d^{-1})			
	JJA	MAM	SON	DJF
Clz.Jac	0.37	0.58	0.31	0.25
Fq.Jac	**0.36**	0.58	0.32	**0.22**
Fq.Med	0.38	**0.57**	**0.29**	0.23
AcKK.Med	0.40	0.59	0.31	0.26
Sub-tropics: 20N to 30N				
Clz.Jac	**0.34**	**0.45**	0.51	0.18
Fq.Jac	0.36	0.46	0.48	0.17
Fq.Med	0.41	0.47	**0.43**	**0.15**
AcKK.Med	0.37	0.48	0.54	0.19
Sub-tropics: -20S to -30S				
Clz.Jac	0.14	0.60	0.38	0.28
Fq.Jac	0.15	0.59	0.38	0.30
Fq.Med	0.14	**0.57**	**0.37**	0.31
AcKK.Med	**0.13**	0.61	0.38	**0.27**
Temperate N: 30N to 60N				
Clz.Jac	0.39	0.51	0.79	**0.19**
Fq.Jac	0.43	**0.49**	0.79	0.20
Fq.Med	0.41	0.50	**0.76**	0.20
AcKK.Med	**0.37**	0.50	0.77	0.20
Temperate S: -30S to -60S				
Clz.Jac	**0.23**	**0.66**	0.35	**0.35**
Fq.Jac	0.24	0.68	**0.32**	0.36
Fq.Med	0.24	0.67	0.33	0.37
AcKK.Med	0.24	0.67	0.34	0.36
Boreal: 60N+				
Clz.Jac	0.38	0.39	0.63	**0.13**
Fq.Jac	0.38	0.39	0.63	0.14
Fq.Med	0.38	0.39	0.62	0.14
AcKK.Med	**0.37**	**0.38**	**0.61**	0.14

Table S7. Latitude mean RMSE by region and season for ET (mm d^{-1}) simulated by each model configuration compared to the GLEAM global ET product.

Tropics: -20S TO 20N	RMSE (ET mm d^{-1})			
	JJA	MAM	SON	DJF
Clz.Jac	0.29	0.50	0.39	0.35
Fq.Jac	**0.28**	0.50	0.40	**0.34**
Fq.Med	0.29	**0.49**	**0.37**	0.35
AcKK.Med	0.31	0.52	0.40	0.37
Sub-tropics: 20N to 30N				
Clz.Jac	**0.22**	**0.23**	0.64	0.18
Fq.Jac	0.24	0.24	0.61	0.18
Fq.Med	0.29	0.26	**0.56**	**0.16**
AcKK.Med	0.25	0.26	0.66	0.19
Sub-tropics: -20S to -30S				
Clz.Jac	0.21	0.80	0.22	0.14
Fq.Jac	0.23	0.79	**0.21**	0.13
Fq.Med	0.21	**0.76**	0.22	**0.12**
AcKK.Med	**0.20**	0.80	0.23	0.13
Temperate N: 30N to 60N				
Clz.Jac	**0.08**	0.46	0.83	0.22
Fq.Jac	0.10	**0.44**	0.82	0.22
Fq.Med	0.12	0.45	**0.80**	0.22
AcKK.Med	0.11	0.45	0.81	**0.21**
Temperate S: -30S to -60S				
Clz.Jac	**0.33**	**0.72**	0.46	0.25
Fq.Jac	0.34	0.74	**0.42**	**0.21**
Fq.Med	0.34	0.74	0.43	0.23
AcKK.Med	0.34	0.73	0.44	0.23
Boreal: 60N+				
Clz.Jac	0.38	0.29	0.59	**0.06**
Fq.Jac	**0.37**	0.29	0.60	0.06
Fq.Med	0.41	0.29	0.58	0.06
AcKK.Med	0.41	**0.28**	**0.57**	0.06

Fig. S11. Colours indicate the JULES model configuration that gives the lowest RMSE compared to either the a) FluxCom or b) MOD17 global GPP (gC m^2 day^{-1}), or c) FluxCom or d) GLEAM global ET (mm day^{-1}) products for DJF over the period 2002 to 2012. Actual RMSE values shown in Fig. S14 and Fig. S15.

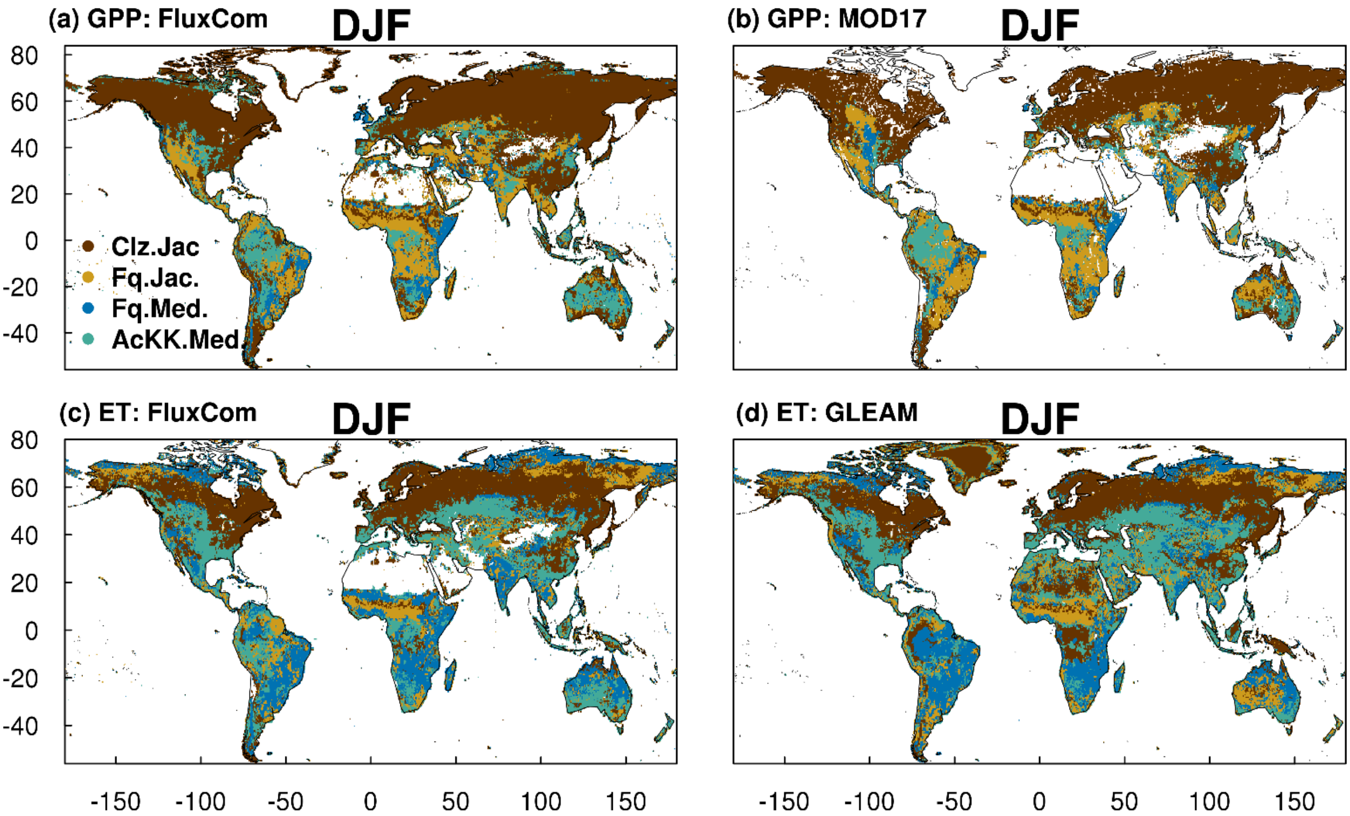

Fig. S12. RMSE of GPP (gC m^2 day^{-1}) in JJA for each JULES model configuration compared to either FluxCom or MOD17 global GPP products.

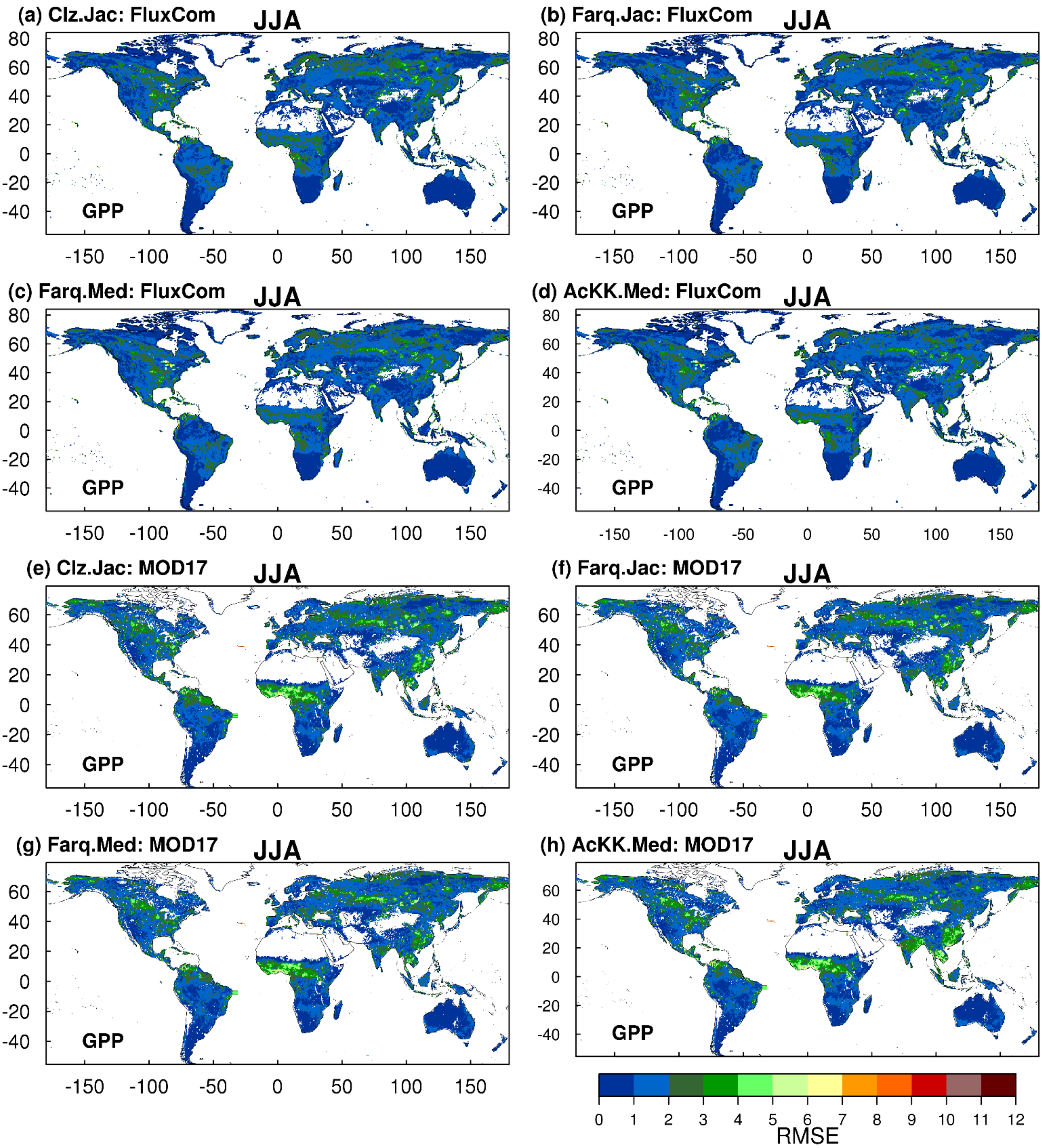

Fig. S13. RMSE of ET (mm day^{-1}) in JJA for each JULES model configuration compared to either FluxCom or GLEAM global ET products.

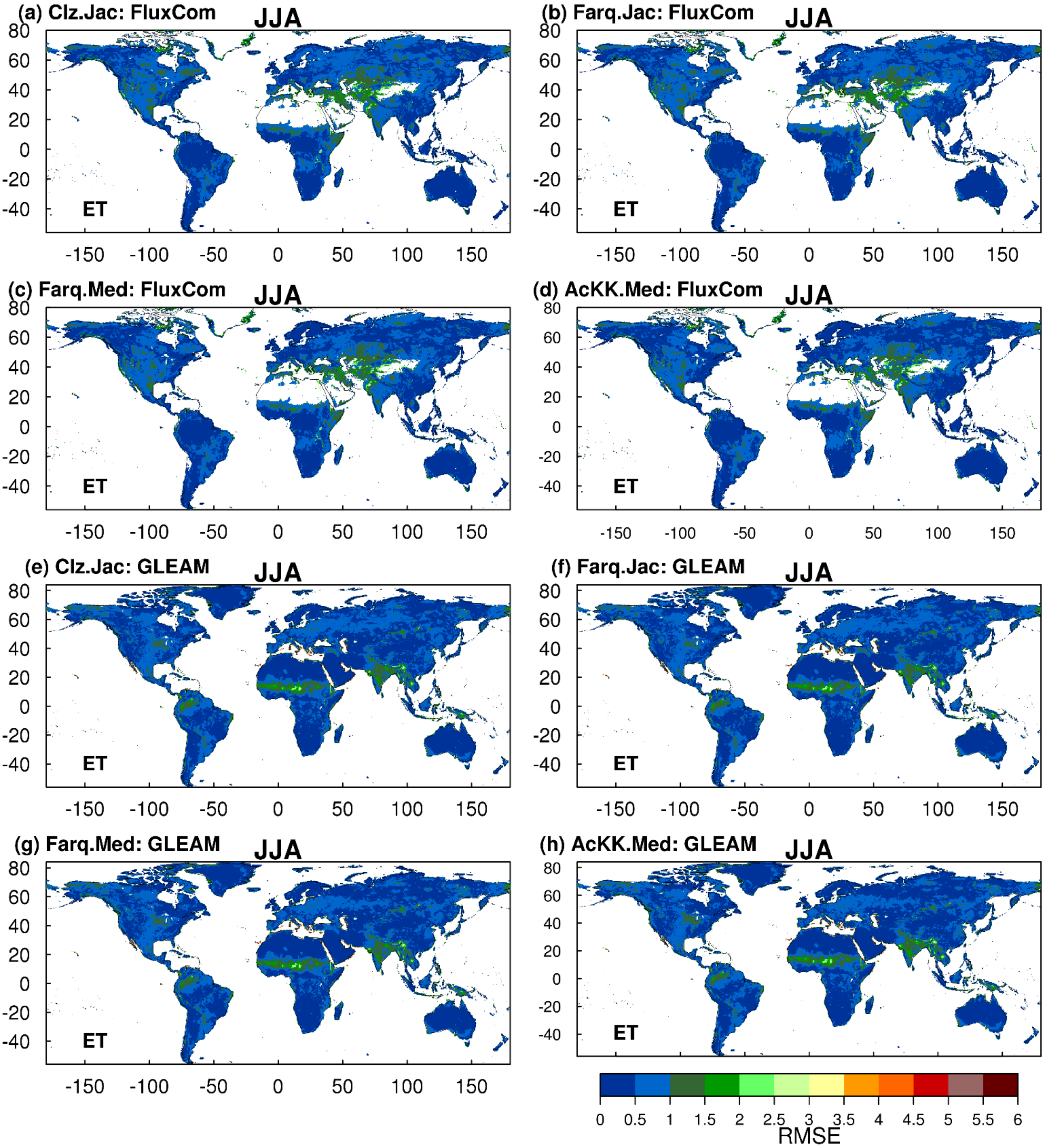

Fig. S14. RMSE of GPP (gC m^2 day^{-1}) in DJF for each JULES model configuration compared to either FluxCom or MOD17 global GPP products.

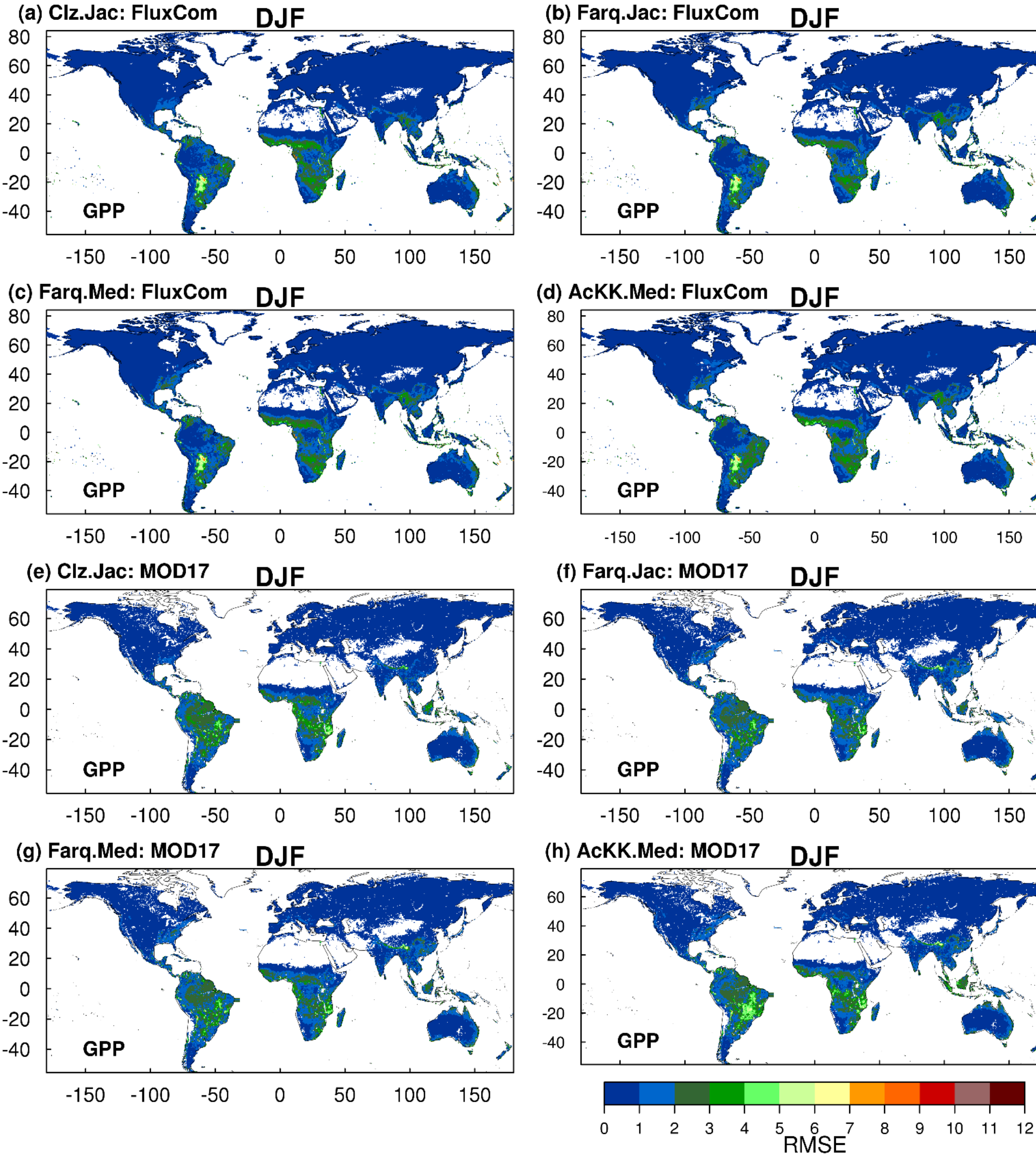

Fig. S15. RMSE of ET (mm day^{-1}) in DJF for each JULES model configuration compared to either FluxCom or GLEAM global GPP products.

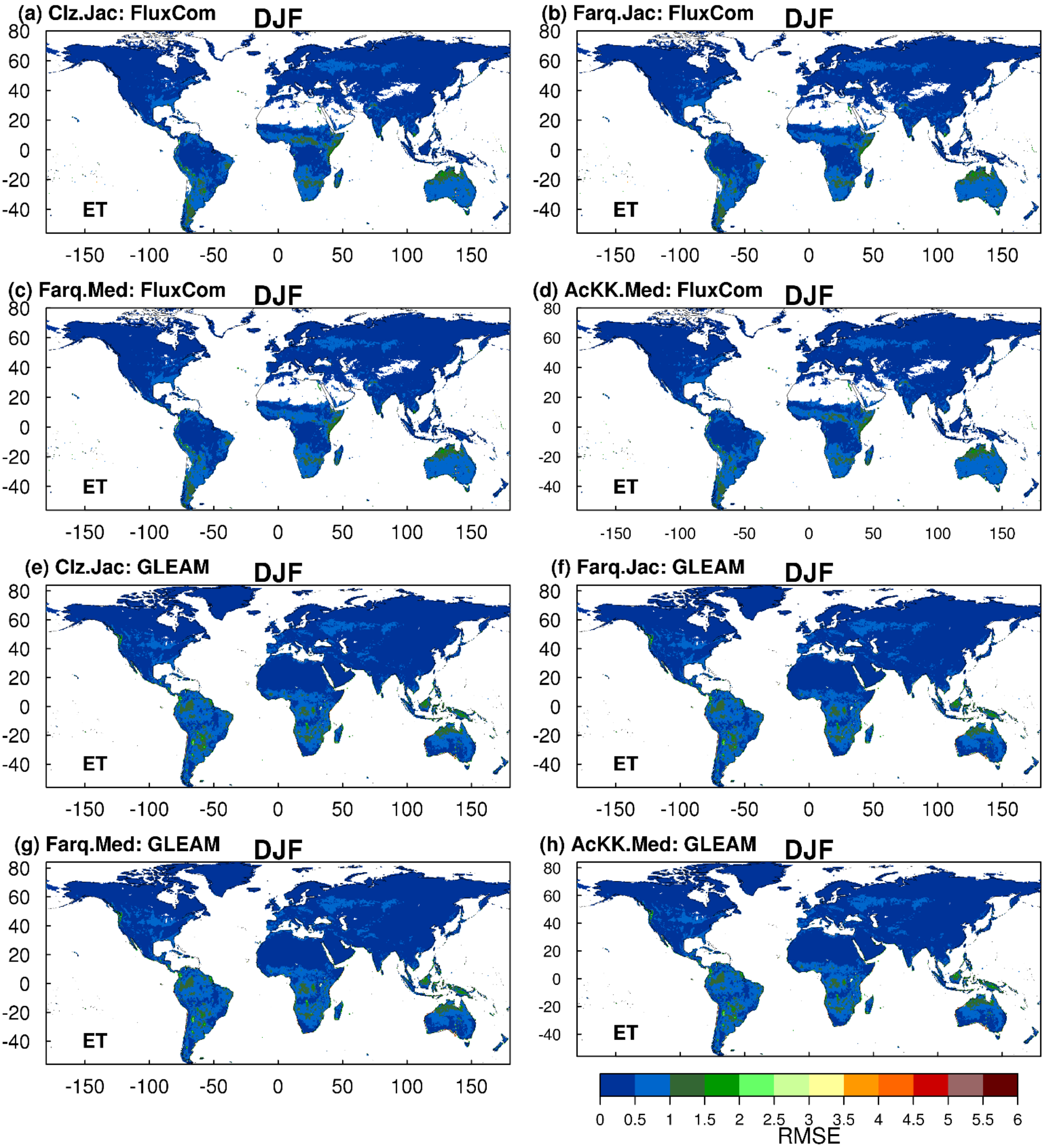

Fig. S16. Change in simulated GPP (g C m^2 day^{-1}), LE (W m^2) and H (W m^2) over the future climate (HadGEM-GC3.1) study period (1980 to 2050) with each model configuration.

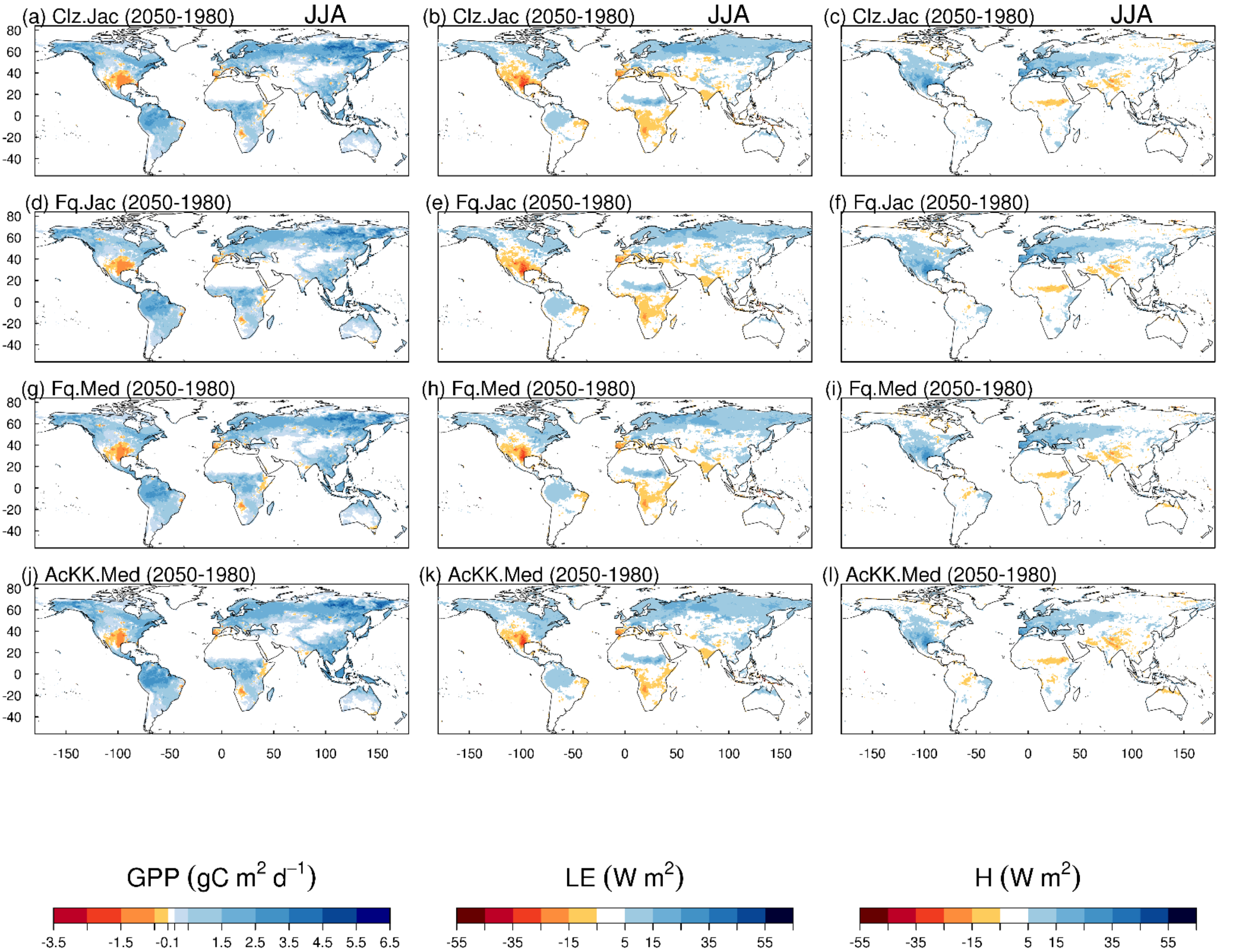

Section S1. Temperature sensitivity in the Collatz photosynthesis scheme as in (Clark et al., 2011)

V_{cmax} at any desired temperature is calculated from the maximum rate of carboxylation of the enzyme Rubisco at 25 ◦C (V_{cmax25}) assuming an optimal temperature range as defined by PFT-specific values of parameters, T_{upp} and T_{low}, as:

$$V_{cmax} = \frac{V_{cmax25}\, f_T\,(T_c)}{\left[1 + \ e^{0.3\left(T_c - \ T_{upp}\right)}\right]\left[1 + \ e^{0.3\left(T_{low} - \ T_c\right)}\right]}$$

Eq. S1

where T_c is canopy (leaf) temperature (◦C) and f_T is the standard Q_{10} temperature dependence:

$$f_T(T_c) = \ Q_{10\_leaf}^{0.1(T_c - 25)}$$

Eq. S2

The default value of Q_{10_leaf} is 2.0.

The photorespiration compensation point, Γ, for C_3 plants is found as:

$$\Gamma = \frac{O_a}{2\,\tau}$$

Eq. S3

Where, τ is the Rubisco specificity for CO_2 relative to O_2:

$$\tau = 2600 Q_{10\_rs}^{0.1(T_c - 25)}$$

Eq. S4

The default value of Q_{10_rs} is 0.57. K_c and K_o are calculated as:

$$K_c = 30 Q_{10\_Kc}^{0.1(T_c - 25)}$$

Eq. S5

$$K_o = 3 \ \times \ 10^4 Q_{10\_Ko}^{0.1(T_c - 25)}$$

Eq. S6

Where, the default value of Q_{10_Kc} is 2.1 and Q_{10_Ko} is 1.2.

References

Clark, D. B., Mercado, L. M., Sitch, S., Jones, C. D., Gedney, N., Best, M. J., Pryor, M., Rooney, G. G., Essery, R. L. H., Blyth, E., Boucher, O., Harding, R. J., Huntingford, C., and Cox, P. M.: The Joint UK Land Environment Simulator (JULES), model description – Part 2: Carbon fluxes and vegetation dynamics, Geosci. Model Dev., 4, 701-722, 10.5194/gmd-4-701-2011, 2011.

Restrepo-Coupe, N., da Rocha, H. R., Hutyra, L. R., da Araujo, A. C., Borma, L. S., Christoffersen, B., Cabral, O. M. R., de Camargo, P. B., Cardoso, F. L., da Costa, A. C. L., Fitzjarrald, D. R., Goulden, M. L., Kruijt, B., Maia, J. M. F., Malhi, Y. S., Manzi, A. O., Miller, S. D., Nobre, A. D., von Randow, C., Sá, L. D. A., Sakai, R. K., Tota, J., Wofsy, S. C., Zanchi, F. B., and Saleska, S. R.: What drives the seasonality of photosynthesis across the Amazon basin? A cross-site analysis of eddy flux tower measurements from the Brasil flux network, Agricultural and Forest Meteorology, 182-183, 128-144, 10.1016/j.agrformet.2013.04.031, 2013.